Multi-omics data integration and network-based analysis drives a multiplex drug repurposing approach to a shortlist of candidate drugs against COVID-19

M Tomazou[1,3,**], M Bourdakou[1,7,**], G Minadakis[1,3,**], M Zachariou[1,3,**], A Oulas[1,3,**], E Karatzas[1,4], E Loizidou[1], A Kakouri[1,3], C Christodoulou[1,3], K Savva[1,3], M Zanti[1,3], A Onisiforou[1,3], S Afxenti[1,3], J Richter[2,3], C G Christodoulou[2,3], T Kyprianou[5,6], G Kolios[7], N Dietis[8], G M Spyrou[1,3,*]

[1]Bioinformatics Department, The Cyprus Institute of Neurology and Genetics, Cyprus

[2]Department of Molecular Virology, The Cyprus Institute of Neurology and Genetics, Cyprus

[3]The Cyprus School of Molecular Medicine, Cyprus

[4]Institute for Fundamental Biomedical Research, BSRC "Alexander Fleming", Vari, Greece

[5]Medical School, University of Nicosia, Cyprus

[6]University Hospitals Bristol and Weston NHS Foundation Trust

[7]Laboratory of Pharmacology, Faculty of Medicine, Democritus University of Thrace, Greece

[8]Experimental Pharmacology Laboratory, Medical School, University of Cyprus, Cyprus

[**] These authors are considered as co-first

[*] Correspondence: georges@cing.ac.cy (GMS)

Research Square

Preprints are preliminary reports that have not undergone peer review. They should not be considered conclusive, used to inform clinical practice, or referenced by the media as validated information.

Abstract

The SARS-CoV-2 pandemic is undeniably the most severe global health emergency since the 1918 Influenza outbreak. Depending on its evolutionary trajectory, the virus is expected to establish itself as an endemic infectious respiratory disease exhibiting seasonal flare-ups. Therefore, despite the unprecedented rally to reach a vaccine that can offer widespread immunization, it is equally important to reach effective prevention and treatment regimens for COVID-19. Contributing to this effort, we have curated and analyzed multi-source and multi-omics publicly available data from patients, cell lines and databases in order to fuel a multiplex computational drug repurposing approach. We devised a Network-based integration of multi-omic data to prioritize the most important genes related to COVID-19 and subsequently rerank the identified candidate drugs. We concluded to a highly informed integrated drug shortlist by combining structural diversity filtering along with experts' curation and drug-target mapping on the depicted molecular pathways. In addition to the recently proposed drugs that are already generating promising results such as dexamethasone and remdesivir, our list includes inhibitors of Src Tyrosine Kinase (bosutinib, dasatinib, cytarabine and saracatinib) which appear to be involved in multiple COVID-19 pathophysiological mechanisms. In addition, we highlight specific immunomodulators and anti-inflamatory drugs like dactolisib and methotrexate and inhibitors of histone deacetylase like hydroquinone and vorinostat with potential beneficial effects in their mechanisms of action.

Introduction

The coronavirus disease 2019 (COVID-19) has claimed, at the time of writing, 877 K lives with more than 26.8 M cases worldwide (WHO - Situation Report ending September 6^{th,} 2020- https://www.who.int/). Despite the unprecedented number of ongoing independent efforts, this global health emergency remains unanswered in terms of effective treatment(s) against COVID-19 and the responsible virus, SARS-CoV-2.

The short-term challenge that needs to be addressed by the scientific community is the realization of therapeutics that can withhold the onslaught of SARS-CoV-2, until vaccines enable mass immunization. The

time scale required for identifying, testing and approving new therapeutic compounds is prohibiting for the urgency of the unfolding situation, albeit more relevant as a medium to long-term response. Thus, the focus is on drug repurposing of existing therapeutics. Yet, even for the case of existing compounds, the experimental pre-clinical screening followed by human safety and efficacy trials is a laborious and time-consuming process. Therefore, prioritization of the candidate drugs entering the testing pipeline is necessary. To this effect, computational approaches can expedite the candidate drug prioritization process through a multitude of methodologies[1] that can exhaustively analyze and integrate the available information on a given drug.

Therapeutics can be categorized roughly into a) those that target the virus itself by blocking its replication and cell entry leading to the reduction of the viral load of the infected patient or reducing transmission, b) those aiming to reverse the effects of the disease such as the acute immune response of the host leading to the well documented cytokine storm and organ damage[2–4] and c) both of the above. Therefore, equally important is the analysis of the disease itself towards deciphering the mechanisms through which COVID-19 develops and progresses.

As the amount of available data accumulates, novel avenues of analysis and informed decisions on drug prioritization emerge. The arsenal of high throughput methodologies (HTS) has already been utilized to produce a diverse space of omics data, originating from clinical and pre-clinical setups from samples derived from human, animal hosts and cell lines. The remaining challenge is on how to integrate the heterogeneous data and extract the critical information needed for selecting potentially repurposable drugs against COVID-19.

In this work, we present a multiplex drug repurposing scheme against COVID-19 via three discrete approaches, stepping on the analysis of multi-source and multi-omics publicly available data from patients, cell lines and databases. Following the drug repurposing approaches, we used a network-based multi-omic data integration approach to prioritize the most important genes related to COVID-19 and subsequently rerank the identified candidate drugs. By combining drug structural diversity filtering along

with experts' curation and drug-target mapping on the depicted molecular pathways, we concluded to an informed integrated shortlist of candidate drugs against COVID-19. The proposed candidates include compounds that were recently found to generate promising results in clinical trials, but also compounds that are presented for the first time in the literature as potential COVID-19 therapeutics.

Results

The workflow adopted in this study outlines five mains steps described in detail below. The overall process entails the analysis of COVID-19 related omics datasets to identify significant genes and protein-protein interactions (PPIs) of interest with the subsequent identification and shortlisting of candidate repurposed drugs (see Figure 1).

Source datasets

During the first part of the analysis we collected publicly available multi-omics datasets released from February to May 2020. These included proteomics and metabolomics datasets from blood serum[5] and seven transcriptomic datasets- four from cultured cell lines (Series 1 - NHBE, Series 2-5- A549, Series 6-A549 with a transduced *ACE2* expressing vector and Series 7-Calu-3)[6], and three patient-derived tissue samples (Series 15 - lung Biopsy, Bronchoalveolar lavage fluid (BALF) and Peripheral blood mononuclear cells (PBMC)[7]. A summary of the data along with the source study is available in Table 3 (see Methods).

Using the log fold-change (logFC) value and *p*-value thresholds (see Methods) from the proteomic dataset, we identified an approximately equal number of over and underexpressed proteins, 62 and 58, respectively. The selected metabolites from the metabolomics dataset included 97 overabundant compounds while the underabundant were approximately 3-fold higher- 317. The analysis of the RNA-Seq datasets yielded 4 sets of differentially expressed genes (DEGs). The PBMC and BALF sets included approximately equal numbers of ~700 over- and ~300 underexpressed DEGs. On the contrary, from the Series 15 set we obtained a relatively large number of 3838 DEGs that were under- against 515

overexpressed DEGs. Finally, the DEG sets from cell-lines (Series 1, 2&5, 6 and 7), included 2588 over- and 1036 underexpressed DEGs in total (Table 3).

In addition, we collected the available information on PPIs between the SARS-CoV-2 and host proteins as reported in Gordon *et al.*, 2020[8] and Human Protein Atlas (HPA) database[9]. This comprised a set of 336 human proteins found to interact with SARS-CoV-2 proteins. For the host-pathogen based approaches (see Methods -PPI Data Selection) we collected 42.7K PPIs across a total of 625 pathogens and human proteins. From the latter, 189 pathogens were found to interact with at least one common host protein with SARS-CoV-2.

Multiplex drug repurposing

We applied 3 discrete drug repurposing approaches based on: (i) transcriptomics, generating 8 lists of candidate drugs, (ii) GWAS-phenotype association (1 list) and (iii) Pathogen-Host PPIs network analysis, generating 3 lists. A summary of all 12 generated lists of candidate drugs is shown in Table 1 while all drugs per list are reported in Supplementary File 3.

i. Drug repurposing based on transcriptomics

Using the RNA-Seq-derived DEG sets, we performed a series of *in silico* drug repurposing analyses with existing computational tools. By selecting the top 150 over- and underexpressed genes with respect to their logFC value (300 in total shown in Supplementary file 1), we obtained two lists of candidate drugs using each DEG set as an input to:

(1) An ensemble of drug repurposing tools: connectivity map [10], L1000CDS2[11] and L1000FWD[12] followed by a scoring process yielding 4 lists with 50 drugs each, namely **Tr1** (from Series 1, 2&5, 6, 7), **Tr2** (from Series 15), **Tr3** (from BALF) and **Tr4** (from PBMC).

(2) CRowd Extracted Expression of Differential Signatures (CREEDS)[13] using the DrugMatrix-based repurposing feature of the tool which maps the expression profile of the DEGs of interest to the effect of

various drugs as measured in rats. By applying the same cutoff of 50 drugs per run we obtained four additional lists- **TrC1** (from Series 1, 2&5, 6, 7), **TrC2** (from Series 15), **TrC3** (from BALF) and **TrC4** (from PBMC).

ii. Drug repurposing based on GWAS – phenotype association analysis

We used 44 genes as input to the PhenoScanner database[14,15]. These genes correspond to 40 strong SARS-CoV-2 interactors according to the evolutionary analysis as reported in Gordon *et al.*, 2020[8] and 4 highlighted proteins ACE2, TMPRSS2, CTSB and CTSL from the HPA database[9].

PhenoScanner identified 480 genetic associations between the input COVID-19-related genes and genes -or proxy genes- previously associated with various phenotypes with a default p-value ≤ 1e-05. Out of these, 186 associations were of genome-wide significance (p-value ≤ 5e-08) with cardiovascular diseases (CVD) being the predominant associated phenotype (Supplementary File 2). Overall, the identified SNP associations corresponded to a set of 83 genes which we used to search for potential drugs in The Drug Gene Interaction Database (DGIdb)[16]. Following this approach, we concluded on a list of 58 drugs (list **GW**) able to target the 83 genes of interest.

iii. Drug repurposing based on pathogen-host interaction network analysis

We worked on the assumption that genetic, functional and morphological similarities between SARS-CoV-2 and other pathogens can be approximated by their taxonomic classification. Drugs with a direct inhibitory effect against a given pathogen are more likely to have a similar effect to closely relate

d pathogens in terms of taxonomic distance. To repurpose drugs based on the above assumption, we derived a taxonomy distance matrix (see Methods) which was used to identify antiviral compounds able to target directly a pathogen proteins according to DrugBank's polypeptide target file[17,18]. This process yielded a list of DrugBank compounds scored as a function of a) the taxonomic proximity of known target-pathogens to SARS-CoV-2 and, b) a metric of the broad-spectrum activity of a given drug. This approach

resulted in a ranked list (**TaxAV**) of 841 antiviral drugs (Supplementary File 5) that were found in DrugBank[17,18] to target a total of 345 unique pathogen NCBI taxonomy IDs.

Building on the above approach, we included the identified PPIs between pathogen and host proteins in an effort to obtain a more informative scoring scheme regarding the functional interactions between pathogens and human. To this effect, we constructed a pathogen-to-pathogen network where edges describe the commonality of each pathogen to SARS-CoV-2 with respect to: (a) their common interactions with host proteins and, (b) the taxonomy distance (see Methods). Herein, the antiviral drugs were scored based on the proximity of target pathogens to SARS-CoV-2, resulting to 1178 (Supplementary File 5) scored drugs (list **HPAV**).

For both TaxAV and HPAV list we selected the top 20 drugs for forwarding to the structural similarity analysis step (Supplementary File 3).

We used the underlying network to screen further for drugs targeting host-proteins. This was based on the assumption that drugs targeting a host protein set with wide interaction overlap between SARS-CoV-2 and other pathogens are deemed more likely to exhibit similar antiviral effects. Herein, drugs were scored by means of a generalized 4-fold equation that accounts for both the host and pathogen protein targets, resulting in a list of 301 drugs. The top 50 drugs (list **HPH)** shown in Supplementary File 3, were selected and forwarded to the drug reranking step, similarly with the other host protein targeting drug lists.

Integration of multi-omic data from patients

We integrated the available multi-omic data from patient samples based on a previously proposed scheme[19]. Specifically, we integrated the following data: (1) ranked DEGs lists in terms of absolute logFC resulting from the transcriptomics data analysis, (2) a ranked gene list in terms of absolute logFC from the proteomics data analysis, (3) a ranked gene list in terms of *p*-value derived from the metabolomics data analysis, (4) an unranked list of host-proteins relevant to viral cell-entry highlighted in HPA[9] and, (5) an unranked list of host-proteins which interact with SARS-CoV-2 from Gordon *et al.*[8].

We calculated the Multi-source Information Gain (MIG) score, a characteristic score per gene comprising the integrated gene-specific information, and the local weighted degree from a synthetic gene-to-gene network based on co-expression, genetic interactions, physical interactions and co-localization extracted from GeneMANIA[20] as described in Methods. We then derived the integrated Multi-source Information (MI) network illustrated in Figure 3 along with the relevant score distributions. The network comprises the top 1000 genes as nodes (specifically 1001 genes due to score ties) originating from all sources with a total of 45486 edges prorating the gene-to-gene relationships.

Finally, for all downstream functional analysis and drug reranking we used the genes ranked based on their MIG score, which represents the integrated gene-disease association.

Highlighting connected pathway communities related to COVID-19 using the generated integration map

We used the top 300 MIG-ranked genes (as described above) to create a map of significant gene-disease associations. Under the guidance of this integrated map, we used PathWalks[21] to allow walkers to cross a pathway-to-pathway network derived from KEGG. The most frequent trajectories highlighted communities of pathways predicted to be widely involved in COVID-19. Using the resulting pathway frequencies *i.e.* number of visits per pathway, we performed an odds ratio (OR) analysis with respect to a random walk using only the topology of the pathway network without any gene map guidance. OR values greater than 1 correspond to higher relative visiting frequency compared to the non-guided runs, and are thus more likely to be involved in COVID-19. The network of highlighted pathway communities is shown in Figure 4.

Reranking of drug candidates based on the calculated target-disease association

The CoDReS tool[22] was used to rerank the candidate drugs based on: (a) a functional score combining the drug targets' relevance to the disease (as captured by the MIG score above), and the binding affinity to its

target genes, (b) an *a priori* score defined as the normalized initial drug ranking from each list, and (c) a structural score representing drugability violations.

We performed the CoDReS reranking on the top 50 drugs with respect to their weighted normalized score, from each of the 10 lists of drugs that target host proteins: 8 from RNA-Seq data, 1 from GWAS and 1 from host-pathogen interactions. The reranked lists are given in Supplementary File 3. Next, we selected the top 20 CoDReS drugs from each list (200 in total) for further analysis.

Filtering drugs with diverse chemical structures

The 200 reranked drugs together with the top 20 candidate antiviral drugs originating from the two pathogen-host interaction based approaches, 240 in total, were screened for chemical structure similarity. Using the ChemBioServer 2.0 we calculated the structural distance matrix based on the Tanimoto index[23], for all pairwise combinations of candidate drugs.

A hierarchical clustering analysis revealed that the input drugs spanned a broad range of chemical structure diversity. Specifically, by applying a distance threshold of <0.2 for highly similar compounds, we obtained 185 clusters, from which 25 comprise more than 1 drug. We eliminated the structural redundancy within our drug list by selecting the top scoring drug from each cluster, yielding a list of 185 drugs. Alcohol was manually excluded as it was deemed inappropriate for pharmacological use against COVID19. Finally, we shortlisted the top 1/3 candidate drugs amounting to 65 candidate drugs which consist the integrated drug list forwarded for evaluation against clinical trials and further curation by experts.

Evaluation of the integrated drug list with respect to ongoing clinical trials

We evaluated further the list of 65 drugs by comparing it against the drugs that are currently in clinical trials against COVID-19 as obtained from clinicaltrials.gov. Specifically, 5 out of the 11 top scoring drugs (dexamethasone, beta-estradiol, atorvastatin, cyclosporin A and remdesivir) are already in clinical trials.

Also, 8 drugs with a lower normalised ranking score (imatinib, hydroxychloroquine, dactolisib, ofloxacin, leflunomide, simvastatin, pioglitazone and methotrexate) were also found in ongoing clinical trials.

From the remaining drugs we identified through structural similarity analysis 2 more drugs which have similar compounds (Tanimoto distance <0.2) in clinical trials. In particular, fluocinoloneacetonide and testosterone were found structurally similar to budesonide and hydrocortisone, which are currently in clinical trials, respectively. The integrated list is shown in Table 2. The detailed table of the integrated list of 65 drugs is presented in Supplementary File 6.

The 65 drugs included in the produced integrated list (Table 2) present a diverse group of compounds from a chemical, pharmacological and clinical perspective. We used three major classification systems to categorize these compounds; the Medical Subject Headings classification (MeSH), the Target-Based Classification (TBC) and the general Chemical classification system (Chem). Although the integrated list contains a versatile group of drugs from a wide range of therapeutic areas (such as anticoagulants, antihistamines and hypolipidemics), the majority of these are antineoplastic agents, followed by immunosuppressive drugs, antivirals and antibacterials. Nevertheless, 16 drugs from the integrated list are experimental drugs, which either are in clinical trials for a number of conditions or are still under pre-clinical investigation. The majority of the drugs in the integrated list are enzyme or protein inhibitors, in terms of their established mechanism of action. Regarding their chemistry, the list is inclusive of important chemical classes of drug molecules such as triazoles, pyrimidines, platinum-containing compounds and benzimidazoles. However, the most prominent general chemical groups in the integrated list were aromatic amines (9 drugs), drugs with at least one piperazine ring (7 drugs), steroids (5 drugs), thiazoles (4 drugs) and quinolines (4 drugs).

A characteristic representation of the drug candidates' classification can be found within the top 5% of their maximum ranking score (between 0.95-1), from which: 11 (65%) are protein inhibitors, 7 (41%) are antineoplastic agents, 5 (30%) are aromatic amines and 4 (24%) include a piperazine ring.

Expert curation and annotation of the integrated drug shortlist

From the integrated list of 65 drugs a thorough expert curation has highlighted a set of 16 drugs (Table 2 and Figure 5). The curation was based on three main criteria: a) drugs that have exhibited evidence of efficacy against COVID-19 in Phase 3 clinical trials; b) drugs that bear pharmacological evidence of direct-targeting of SARS-CoVs molecular components; and c) clinically approved drugs that have activity in molecular pathways that have been shown in the literature to be implicated in SARS-CoV-2 biology.

The first criterion yielded 2 drugs from the integrated list, dexamethasone and remdesivir, which are the only drugs that have shown to be effective against COVID-19. Nevertheless, from these two, only remdesivir has shown a direct effect against SARS-CoV-2, whereas dexamethasone showed an effect in the reduction of the associated inflammation of the disease rather than the biology of the virus.

The second criterion of the curation yielded 6 experimental drugs from the integrated list, which have shown a direct effect on SARS-CoVs in various assays (mostly in vitro). Benzyl (2-oxopropyl) carbamate, D3F, F3F, GRL0617 and WR1 have shown direct inhibition of the coronavirus replicase polyprotein 1ab[24–28] (https://pubchem.ncbi.nlm.nih.gov/bioassay/[Bioassay Number], Bioassay Numbers: 977608, 1811, 977608, 977610), which is a major viral protein for the viral replication machinery[8]. N-(2-aminoethyl)-1-aziridineethanamine has shown direct inhibition of the human Angiotensin I converting enzyme 2 (ACE2) receptor[29,30].

The third criterion yielded 9 clinical drugs from the integrated list. These drugs were shown to be effective in targeting SARS-CoV-2 replication cycle and more specifically processes implicated in the generation of virally encoded non-structural proteins (NSPs) which are essential for the assembly of the viral replicase complex. Vorinostat and hydroquinone are histone deacetylase (HDAC) inhibitors; it has been proposed that the main viral protease (Nsp5) may inhibit HDAC2 transport into the nucleus and therefore HDAC2 inhibitors may be able to disrupt this interaction and suppress the HDAC2-mediated inflammation and interferon activation[8].

Some HDAC inhibitors have been shown to have antiviral activity (such as HDAC6 inhibitors against Influenza A Virus)[31] and there is considerable literature that links HDAC inhibitors with T-cell biology and the immune response[32,33]. Bosutinib, dasatinib, imatinib and saracatinib are tyrosine kinase inhibitors; tyrosine kinase-linked pathways have been implicated in SARS-CoV-2 biology and activation[34], with various inhibitors having a potential anti-SARS-CoV-2 efficacy. Interestingly, dasatinib and imatinib have previously shown inhibitory effects against the MERS and SARS-CoV viruses *in vitro* at micromolar concentrations[35], as well as against SARS-CoV-2[36,37]. Their wide antiviral efficacy has also been showcased against HIV[38]. Methotrexate is a drug with a strong effect in nucleic acid synthesis and a multi-facet role as antineoplastic, antimetabolite and antirheumatic drug. Interestingly, it was recently shown to present a sub-micromolar activity against SARS-CoV-2, *in vitro*[37]. Finally, dactolisib is a drug with a dual activity as a PI3K/mTOR inhibitor, a pathway that we know is important in SARS-CoV biology[39,40]. Although there is evidence of the antiviral activity of the above drugs against HIV[41], their potential efficacy against SARS-CoVs is yet to be determined.

Discussion

Mounting evidence indicate that the clinical manifestations of COVID-19 are systemic, affecting mainly the respiratory and digestive tract, the cardiovascular but also the Central Nervous System (CNS)[42–46]. Thus, we pursued an approach that integrates multi-omics data from different types of tissue (BALF, PBMC, alveolar, NHBE, Calu-2 cell lines and blood serum) aimed to build a comprehensive molecular profile of the disease to obtain a more informative basis for drug repurposing. Across the most significant DEG sets selected for the integration step we observed minimal overlap (24 out of 1K selected - 2.4%) indicating a complex perturbation scheme involving a broad range of biological pathways across different tissues and further supporting the need of a multi-source approach.

Coming from patients with severe COVID-19, the identified DEG sets were as expected enriched with genes that are involved in acute immunoresponse and inflammation. Specifically, the top MIG scoring

inflammation factors SAA1/2 and CRP were previously proposed as severity biomarkers for the disease[47] and as indicators of inflammatory tissue damage. Cytokine release related factors, such as CCL3/4, CXCL10, CLC, IL2R and IL10 were also highly ranked along with p53 apoptosis pathway related genes NTRK1, CTSL, CTSB and IGFB[7]. Genes involved in complement activation and coagulation cascades such as C4a and C5 were also highly perturbed likewise with past *Betacoronaviruses* related outbreaks(SARS and MERS)[48]. The FDCSP, KCNJ2 and ST20 reported to be highly dysregulated from lung biopsies[49] along with FLNA and EGFR point to significant effects of COVID-19 in lung and gastrointestinal epithelia cell proliferation signaling. Specifically the latter (EGFR) has sparked a wider discussion on the involvement of growth factor receptors in viral infections and potential drug repurposing avenues of related antineoplastic compounds[50,51].

The composition of the identified DEG sets and the functional analysis performed in Pathwalks highlighted several pathways related to immune and inflammatory response pathways. Namely, in the top 30 scoring KEGG pathways (Figure 4) with respect to their OR values, we highlighted the *Complement and coagulation cascades, IL-17 signaling pathway, Chemokine signaling pathway, Cytokine-cytokine receptor interaction* and *Fc epsilon RI signaling pathway*. The *Renin-angiotensin system* and *Renin secretion* pathways were also highlighted as a result of the central role of ACE2 in viral entry along with the genes involved in the coagulation cascades[52]. In addition, we found a number of mechanisms involved in more generic KEGG disease terms that are related to infections and respiratory conditions like in *Pertussis, Asthma, Staphylococcus aureus infection, Prion diseases, Malaria, Systemic lupus erythematosus* and *African trypanosomiasis*.

In line with the above COVID-19 molecular profile, 9 candidate drugs in our proposed integrated list are classified (MeSH) as anti-inflammatory and immunosuppressors such as dexamethasone, cyclosporinA, mercaptopurine, cytarabine, fluocinoloneacetonide, triptolide, LY-255283, tegafur and methotrexate. These were complemented by the Non-Steroid Anti-Inflamatory Drugs (NSAID), bromfenac, zileuton, rofecoxib and choline salicylate. The anticoagulants, renin-angiotensin system targeting drugs in the list were Y-27632, calcium citrate and the ACE2 targeting N-(2-aminoethyl)-1-aziridineethanamine and

hydroxychloroquine. Several drugs from the integrated shortlist are classified as antineoplastic/anti-proliferative agents (20 in total) including vorinostat, bosutinib, dasatinib and others. While the antineoplastic drugs are expected to arise from such repurposing approaches which inevitably identify key genes in proliferation signaling(e.g. EGFR) and apoptosis (p53 signaling pathway) there is a growing interest in the use of this class against viral infections[50,51].

Focusing on the experts' curated shortlist from a pathophysiological perspective, a group of four drugs bosutinib, dasatinib, cytarabine, saracatinib are of particular interest as their primary mechanism of action is mediated by the inhibition of Src Tyrosine Kinase. Inhibiting the latter could help COVID-19 patients who enter a severe clinical trajectory through a number of pathophysiological mechanisms recognized to be involved from pre-clinical and clinical studies either directly involving COVID-19 or based on previous observations and experiments:

a) Bruton's tyrosine kinase (BTK) signaling has been associated with the production of proinflammatory cytokines that can contribute to COVID-19 immunopathology, T-cell differentiation, function, and survival, hence might be beneficial in treating COVID-19 related immunopathology and lymphopenia[53] . This has been already tested in clinical trials[54] and for dasatinib it has been confirmed from seminal studies in chronic myelogenous leukemia[55].

b) Tyrosine Kinase inhibitors, have been used to inhibit platelet function (antithrombotic activity) through several mechanisms including novel mechanisms like GAS6/TAM signal inhibition, targeting the MERTK tyrosine kinase active site with a highly potent and bioavailable MERTK inhibitor, UNC2025[56].

c) Mechanical ventilation (MV) has been extensively used to support patients with COVID-19 pneumonia who are developing respiratory failure; however, mortality is unexpectedly high, higher than current ARDS mortality from other etiologies. It has been confirmed from in-vitro, ex-vivo and *in-vivo* studies that MV itself can induce lung injury through inflammatory Src Tyrosine Kinase signaling, ICAM-1 expression, leukocyte infiltration, and vascular hyperpermeability[57]. Pulmonary vascular endothelial barrier function is indeed, partially regulated by Src kinase-dependent phosphorylation of caveolin-1 and intercellular adhesion molecule-1. Blocking these mechanisms with Src tyrosine inhibition (*i.e.* nintedanib[58]) has proved

effective in preventing acute lung injury (ALI) in animal studies including the potentiation of bleomycin-induced ALI[59] .

d) Pulmonary ischemia–reperfusion (IR) which is associated with a wide range of clinical events[60], including lung transplantation, cardiopulmonary bypass, trauma, resuscitation for circulatory arrest, atherosclerosis, and pulmonary embolism and pulmonary embolism, the latter being widely recognized as a detrimental complication of severe COVID-19[61].

e) A final mechanism by which Tyrosine Kinase Inhibitors could possibly exert anti-COVID-19 action is by eliminating excess soluble fms-like Tyrosine Kinase (in blood) which has been correlated with endothelial dysfunction and organ failure in critically ill COVID-19 patients[62,63].

Complementary to the Src Tyrosine Kinase inhibitors, the interest on hydroquinone and vorinostat stems from the fact that melanin synthesis inhibition (e.g. by hydroquinone) involves similar pathways with Tyrosine Kinase. Both drugs are inhibitors of Histone deacetylase and have been used to treat pediatric brain cancers[64] and might exert a beneficial effect through inhibition of the pro-inflammatory cytokine storm progression. While vorinostat has been used against HPV[65], we have not found any specific references in the current literature linking this drug category to COVID-19.

Inhibitors of class IA phosphatidyl inositol-3 kinases (PI3-K), such as dactolisib, are targeting immune responses, particularly through co-stimulation by CD28 and ICOS and have been reported to suppress clinical symptoms in ongoing experimental autoimmune encephalomyelitis (EAE) and inhibited MOG-specific responses *in vitro*[66]. Hence, the latter class of drugs can be beneficial in treating COVID-19 effects to the CNS albeit the underlying mechanisms and the pathology are not well understood. On the other hand, activation of PI3K/Akt pathway has been reported to cause attenuation of ER stress-induced myocardial apoptosis, facilitating the NGF induced heart protection[67]. Given that myocardial involvement in COVID-19 was observed in a subset of patients and has detrimental consequences, there might be a reason to be cautious how we interpret this finding.

Despite being less studied, the identified compounds that target directly the viral entry and replication mechanisms and related proteins are of interest. Through our pathogen network based approaches the integrated list of antivirals comprises remdesivir, the first drug to obtain FDA approval for emergency use in patients with severe COVID-19[68], along with a number of experimental compounds developed during the SARS and MERS outbreaks with promising *in vitro* results such as benzyl (2-oxopropyl)carbamate[69,70], D3F, F3F, GRL0617 and WR1. This list is also complemented by N-(2-aminoethyl)-1-aziridineethanamine that can be effective *via* its inhibition of ACE2 which is being used by SARS-CoVs for cell entry in order to initiate membrane fusion and cell infection[71]. As expected, the top scoring antivirals repurposed based on commonality and available information from other pathogens were the ones known to be effective against the closest taxa e.g. members of the SARS-CoV species. However, our full lists of antiviral drug rankings (HPAV and TaxAV available in Supplementary File 5) identified and reranked drugs nearly from all main phyla of viruses but also from bacteria that may share interactions with the same host proteins or share genetic similarity. In fact, this approach which was developed and utilized herein specifically for SARS-CoV-2 introduces a rapid mapping and prioritization method of all the known anti-viral compounds against any pathogen of interest.

Concluding, we have identified a shortlist of drugs generated from multi-source, multi-omics data utilizing a multiplex drug repurposing approach. Note that, we do not anticipate that a single drug can lead to a sufficiently effective treatment of severe COVID-19 and especially in patients with comorbidities. Based on the multi-faceted nature of COVID-19, an effective treatment will require combination(s) of drugs, allowing to target multiple pathways to provide a) anti-inflammatory effects to prevent collateral tissue damage b) inhibition of the viral replication mechanisms and c) where required, protective effects which account for other underlying conditions like cardiovascular disease. We anticipate that the proposed integrated list of drugs will enhance the underlying rational and provide insights from a molecular point of view for the compounds that have already entered clinical trials and more importantly will point towards novel therapeutic avenues involving the newly proposed ones.

Methods

Multi-omics and PPI data selection and preprocessing

The number of differentially expressed genes, proteins and metabolites with their corresponding selection criteria are shown in Table 3 and were derived as follows:

Transcriptomics

Transcriptomic (Expression profiling by high throughput sequencing) data were obtained from Gene Expression Omnibus accessed on 9 April 2020 with id GSE147507[6]. This dataset consists of transcriptional profiling of different cell lines with SARS-CoV-2 infection and of transcriptional profiling of COVID-19 lung biopsies. In our study we used independent biological triplicates of primary human lung epithelium (NHBE), transformed lung alveolar (A549) and transformed lung-derived Calu-3, which were mock treated or infected with SARS-CoV-2. We also used independent biological copies of the transformed alveolar lung (A549) that were transported with a carrier expressing human ACE2, which were also mock treated, or were infected with SARS-CoV-2. Finally, we included uninfected human lung biopsies from two patients that were used as biological replicates and lung samples derived from a single COVID-19 deceased patient that was treated in technical replicates. Differential expression analysis of the RNA-Seq data was performed in R programming language using the EdgeR package[72]. We removed low expressed genes by retaining only those genes that are represented at least in two samples of each group. The mRNA counts were normalized using the trimmed mean of M-values (TMM) method. Finally, we used EdgeR's negative binomial model to perform the differential expression analysis of infected compared to control samples. From the comparisons we selected the differentially expressed genes (DEGs) by applying selection thresholds of adjusted p-value < 0.05 and logFC >= 2.

In addition, we included RNA sequencing data of RNAs isolated from bronchoalveolar lavage fluid (BALF) and peripheral blood mononuclear cells (PBMC) specimens of COVID-19 patients[7]. Specifically, this dataset

included two BALF samples from Zhongnan Hospital of Wuhan University and three BALF samples from healthy controls, downloaded from the NCBI SRA database with accession numbers: SRR10571724, SRR10571730, and SRR10571732. PBMC samples from 3 COVID-19 patients and 3 healthy donors were obtained from Zhongnan Hospital of Wuhan University (Table 3). From these sets, DEGs were selected based on the original publication analysis as described in Xiong*et al.* 2020[7]. Specifically, DEGs had been identified using the DESeq2 package (v1.26.0)[73]. Selection thresholds on BALF derived DEGs were set at FC >= 4, and adjusted p-value < 1e-10 and at least 10 read counts on average across all samples. For the PBMC data, due to lower sequencing depth the DEGs were selected using FC >= 2, adjusted p-value < 0.01 and over 100 read counts on average across all samples.

Proteomics and metabolomics

To further enrich our study, we included proteomic and metabolomic data from Shen *et al*.2020[5]. In this study, the authors performed proteomic and metabolomic profiling from sera of COVID-19 and healthy individuals. These samples were procured from 65 patients who visited Taizhou Hospital from January to March 2020. They were diagnosed as COVID-19 according to the Chinese Government Diagnosis and Treatment Guideline. From the analysed proteomic and metabolomic profiles, 28 severe COVID-19 patients and 28 healthy controls were used in our analysis and more specifically the differentially abundant proteins and metabolites, based on adjusted p-value < 0.05 and absolute logFC > 0.25 reported by the authors using a Two-sided unpaired Welch's t-test.

Mapping between metabolites and genes was performed using the Ingenuity Pathway Analysis (IPA) software by Qiagen[74](http://www.ingenuity.com). HMDB IDs, logFC and p-value were used as input into the IPA software which identified the upstream regulators (Supplementary File 1) that may up-regulate or down regulate the input metabolites. The right-tailed Fisher's exact test was to obtain the p-values of the identified regulatory genes.

PPI data selection

A set of 336 SARS-CoV-2-human proteins, available in the Human Protein Atlas (HPA) repository, have been further employed in the study. Specifically, the set involves 332 high-confidence SARS-CoV-2-human PPIs, identified by Gordons et al. (2020)[8], who had cloned, tagged and expressed 26 SARS-CoV-2 proteins in human cells, by means of affinity-purification mass spectrometry (AP-MS). Four additional proteins were included: the ACE2 receptor used by SARS-CoVs for host cell entry[52,75], the serine protease TMPRSS2 involved in the S protein priming[52] and the endosomal cysteine proteases cathepsins CTSB and CTSL needed for viral cell entry, which have been widely expressed in human tissues[52,75].

PPIs between host and pathogens other than SARS-CoV-2 were downloaded from Intact[76], PHISTO[77] and VirHostNet[78] amounting to a total of 42684 unique PPIs from a total of 625 organisms.

Drug repurposing pipelines

i. Transcriptomic-based drug repurposing

The transcriptomic-based drug repurposing was performed based on human cell lines and *ex vivo* (rat liver) drug repurposing tools. The 150 over and under expressed genes (based on their FC value) from the BALF, PBMC, Series 15, 1, 2, 5, 6 and 7 were used as transcriptomic signatures. The expression data from series 2 and 5 were pooled and analyzed prior to the drug repurposing rans in a single set since they were generated from the same cell lines and treatments. Next, each set was used as an input in three different transcriptomic-based computational drug repurposing (DR) tools: Connectivity Map[10], L1000CDS2[11] and L1000FWD[12]. These tools use transcriptional expression data from multiple human cell lines, to probe relationships between diseases and therapeutic agents. Drugs are sorted according to their "enrichment" score, which characterizes if a drug can enhance or reverse the expression levels of a disease based on a given set of genes. Drugs with high negative scores are those that can reverse the gene expression profile towards the normal state.

For each input set we obtained a candidate list of drugs predicted by each of the three tools, ranked based on their respective reverse enrichment score (inhibition score). Next, the top 50 drugs from each of the three

tools were combined as their union of unique drugs, and ranked by calculating the weighted sum of normalized average rankings and the normalized number of appearances according to formula (1):

$$Score_i = w_1 * R_i + w_2 * A_i,\ i = 1, \ldots, N\ drugs \quad (1)$$

where R_i is the average ranking score from each of the three tools, A_i the number of appearances of each drug in the three DR tools and w_1 and w_2 0.7 and 0.3, respectively.

The drug lists obtained from Series 1, 2&5, 6 and 7 sets were combined and reranked again using formula (1) in order to conclude to a single drug list from all cell line derived RNA-Seq data.

The same gene expression sets were used as input to the CRowd Extracted Expression of Differential Signatures (CREEDS) gene and drug perturbation database[13]. The CREEDS database consists of a list of 4295 single drug perturbations and 8620 single gene perturbations obtained using gene expression data from different tissue types of rat, collected from GEO. The CREEDS database was used herein to extract drugs from the DrugMatrix [13] that are predicted to be able to reverse the disease expression profile of the gene sets of interest. The drugs are ranked by the tool based on Fisher's exact test derived p-value. Like above, the top 50 drugs based on the enrichment score returned by CREEDS. Again, the candidate drugs obtained from series 1, 2&5, 6 and 7 were combined and ranked according to formula (1).

Table 1 shows a summary of the 8 drug lists (**T1-4, TC1-4**) obtained from RNA-Seq data.

ii. GWAS/phenotype-related COVID-19 drug-repurposing

The 40 strong SARS-CoV-2 interactors according reported in Gordon *et al.*[8] were used as an input to PhenoScanner[14,15]. PhenoScanner returns genotype-phenotype associations across traits and proxies that are collected from various other online databases such as GWAS catalog[79] and CHARGE[80].

Phenotype-associated genes were extracted automatically from Phenoscanner and were used to search for drug interactors. More specifically, the genes were used as input to the drug–gene interaction database -

DGIdb (www.dgidb.org)[16] which consolidates, organizes and presents drug–gene interactions and gene druggability information from papers, databases and web resources.

iii. Pathogen network-based drug repurposing

Pathogen identification and taxonomy-based distances

From the polypeptide targets datafile of Drugbank we extracted the NCBI taxonomy[81] IDs of all organisms other than *Homo sapiens* contained in Drugbank[17,18] and have at least one protein that is targeted by a drug. This set was filtered to identify and remove non-pathogens like *Metazoa* and plants using a custom written script in R in combination with the taxize package to retrieve the taxonomy classification of the organisms. The final list of pathogens included viruses, bacteria and known human parasites from eukaryotes. From the resulting pathogen tax id list we constructed their taxonomy tree using R's taxize package[82]. The distance between each node was calculated using a variable step size between taxonomy ranks proportional to the loss of information at each level as previously proposed[82–84].

Drug repurposing using the taxonomy distance matrix

Building on the taxonomy-derived pathogen-to-pathogen similarity we have assumed that the likelihood of a given drug with a known protein target, to have other protein targets in other organisms is higher for shorter taxonomy distances.

In addition, drugs with protein targets across a broad and diverse range of taxonomy distances are more likely to have a less taxon-specific effect raising the prospect that they are repurposable against SARS-CoV-2, as opposed to drugs known to target only a specific group of distant pathogens. This broad spectrum anti-pathogenic activity can be captured by the maximum distance of organisms affected by the same drug, while the diversity in the inter-taxon distances can be captured using the Shannon Index *H* i.e. entropy.

Using the above we have scored drugs based on function (2):

$$S_x = \max_{i \in R_x} \frac{1}{d_i} + a \cdot H \quad (2)$$

Where *Rx* is the set of *n* pathogens with known protein targets for drug *x*, *di* is the taxonomy distance of the *ith* pathogen targeted by drug *x*, and *α* the maximum difference of distances d across the pathogens in set *Rx* which can be written as:

$$a = \max_{i \in R_x, j \in R_x} |d_i - d_j| \quad (3)$$

Finally, the Shannon diversity[85,86] of distances *H* can be expressed as:

$$H = \sum_{z=1}^{D_x} p_z ln\, p_z \quad (4)$$

Where *Dx* is the set of discrete distance values observed in *Rx* while *pz* is the ratio of the distance *dz* frequency over the total number of measured distances in *Rx* (equal to n-1).

Sx is maximized as d_i approaches 0 but for larger distances a drug is favored over other equidistant drugs if it is found to have protein targets over a broader and diverse range of pathogens.

Pathogen-host PPI network-based drug repurposing

The approach in this section draws from the assumption that similarities between SARS-CoV-2 and other pathogens at host-protein level, may provide the appropriate framework to identify and rank candidate drugs to be used against COVID-19. Specifically, a database repository was initially developed by collecting and combining all the protein and host-protein interactions from all organisms found in IntAct[76], Phisto[77] and VirHostNET[78] data repositories. The pathogens were identified from the combined unique list of NCBI taxonomy[81] IDs from the aforementioned databases and filtered for non-pathogenic organisms like above. For the case of SARS-CoV-2 pathogen, the 366 host-proteins found in HPA[9] were used, where a pairwise pathogen-to-pathogen network was developed based on common host-proteins in-between pathogens. Herein, the node size represents the number of host-proteins related to a specific pathogen, and the edge weight represents the number of common host-proteins in-between two pathogens. The underlying network revealed 189 pathogens that share common host-proteins with SARS-CoV-2, forming a network of first-neighbors. Based on the assumption that the relation between two pathogens cannot be approximated only

by their observed commonality at host-protein level but also by the previously mentioned taxonomy distance D in-between them, the latter network was further enriched with an additional edge score (S_{edge}), according to the following equation:

$$S_{edge} = \frac{2N_{com}N_{min}(1-D)}{(N_1+N_2)\,N_{max}10^{\left(\frac{1}{N_{com}}\right)}} \quad (5)$$

where N_1, N_2: The number of host-proteins interacting with the two pathogens forming a single edge. N_{com}: The number of common host-proteins that two pathogens share. N_{min}, N_{max}: The maximum and minimum estimations of $v = \{N_1, N_2\}$vector. D: The taxonomy distance between two pathogens.

Herein, the final ranked drug list comes from a specific methodology that scans the edges of the underlying SARS-CoV-2 sub-network, one by one. Specifically, for each pair of pathogens, drugs were obtained from DrugBank, which target the common host-proteins that form the specific edge. Each drug in the list was ranked according to the following generalized 4-fold equation:

$$S_{drug} = 0.25\left(\frac{N_{vtar}}{N_1} + \frac{N_{vtar}}{N_{dtar}} + \frac{N_{xtar}}{N_2} + \frac{N_{xtar}}{N_{dtar}}\right) \quad (6)$$

where, N_{vtar} is the number of drug targets included in SARS-CoV-2 host-proteins, N_{xtar} is the number of drug targets included in the x-pathogen that forms an edge with SARS-CoV-2, N_{dtar} is the total number of drug targets that derive from DrugBank repository[17,18], N_1, N_2 is the total number of host-proteins included in SARS-CoV-2 and the x-pathogen accordingly. The overall drug score was then obtained by combining equations (5) and (6) as follows:

$$S_d = \left[\left(\frac{UN_{tar}}{2N_1}\right) + \left(\frac{\sum_{i=1}^{N_{app}} S_{drug}(i)}{2N_{app}}\right)\right] \times \left(\frac{\sum_{i=1}^{N_{app}} S_{edge}(i)}{N_{app}}\right) \quad (7)$$

where, N_{app} is the number of times a specific drug appeared through the scanning process, UN_{tar} is the number of unique targets appeared in the scan process, N_1 is the number of SARS-CoV-2 host-proteins used, and S_{edge}, S_{drug} are the estimated scores per edge obtained from (5) and (6) equations accordingly.

Multi-omic data integration

Towards the integration of multi-source data from patient samples, we developed a *network-based multi-source data integration* methodology based on the integration scheme presented in Zachariou et al. 2018[19].

Data pre-processing

We integrated data from multiple sources in the form of gene lists with two columns, corresponding to gene identity and gene score from the following sources and shown in Supplementary File 1:

1. ranked genes lists in terms of absolute logFC from three serum transcriptomic (T) datasets (Series 15, BALF, PBMC)[6],
2. ranked genes lists in terms of absolute log fold from one proteomics (P) dataset[5]
3. ranked genes lists in terms of p-value from one metabolomics (M) dataset[5]
4. unranked list of host proteins (PPI) which interact with SARS-CoV-2 from Gordon et al.[8]
5. unranked unique gene list from HPA, excluding the genes identified in Gordon et al.

The gene symbols in all the gene lists were converted to entrez ID for consistent merging to a single gene ID using the R package org.Hs.eg.db[87] for genome wide annotation for Human. For the three transcriptomics and the proteomics data set, the gene score GS_x per list was calculated based on:

$$GS_x = \frac{L_x-(R_x-1)}{L_x} \qquad (8)$$

where L_x is the total number of genes per list and R_x in the rank of each gene based on their absolute log FC $x \in \{T, P\}$ and for $x \in \{M\}$ based on their p-value. GS_x is in canonical form as it takes values $GS_x \in (0,1]$ for all gene lists. For the two lists from HPA and Gordon et al. (PPI) their gene score was assigned to 1.0 for all genes.

The three transcriptomic gene lists were merged and the final score per gene was assigned to be the average $GS_x,\ x \in \{Series15, BALF, PBMC\}$ across the three datasets.

Gene-Gene Synthetic Network and Gene Prioritization

We calculated a characteristic score per gene, known as the Multi-source Information Gain (MIG) comprised by two parts,

$$MIG = w * MIG_n + (1 - w) * MIG_e \text{ (9)}$$

where MIG_n represents the normalized integrated n^{th} gene-specific information (i.e. node characteristics) and MIG_e represents the normalised integrated gene-gene information (based on the topology of the multi-integrated super network) and corresponds to the weighted degree of the multi-integrated super network. We considered equal contribution to the score of the gene-specific information and of the topology of the integrated gene-gene super network ($w = 0.5$).

The gene-specific information is given by

$$MIG_n = \sum_i \ w_i V_i, i \in \{T, P, M, PPI, HPA\} \qquad (10)$$

where V_T is a vector corresponding to the average gene score of the three transcriptomic datasets (Series 15, BALF, PBMC), V_P is a vector corresponding to the scored gene list from the proteomics, V_M is a vector corresponding to the ranked genes from the dataset, V_{PPI} is a list of unranked genes corresponding to the set of proteins as identified from Gordon et al. 2020[8] and V_{HPA} is a list of unranked genes corresponding to the unique proteins annotated to be key in the HPA excluding the V_{PPI} ones.

The weights w_x^n for the respective sources were set to ensure that at least 20% of each gene list is included in the top 500 genes. In addition, the weights were set so that their sum satisfies the condition:

$$\sum_i w_i = 1 \, , i \in \{T, P, N, HPA, PPI\} \quad (11)$$

The integrated gene list contained in total 1351 genes. We filtered to retain only the genes which were recognizable by the GeneMANIA tool resulting in a list of 1118 genes. From that we selected the top 1000

top scored genes based on their integration score to build networks using the GeneMANIA tool[20] in Cytoscape[88]. Note that 1001 genes were selected as three genes shared the same score at the bottom of the list. We selected four networks in GeneMANIA based on co-expression, co-localization, genetic interaction and physical interaction.

The Multi-source Information (MI) super network was constructed based on the weighted sum of the pairwise weighted edge vectors (for each pair of genes) for these four types of networks (the edge weight automatically calculated by GeneMANIA). The total number of connected nodes out of the 1001 genes was 995 and the total number of edges 45486.

By combining both the nodal and the topological information using equation (10) we calculated the final gene score MIG and ranked the genes with respect to their importance and involvement in COVID-19 based on that (Supplementary file 4).

The igraph package[89] in R[90] was used to generate and analyse the MI super network and to compile the MIG score.

Functional analysis and pathway community identification

Pathwalks[21], a map-driven random walk-based methodology on a pathway-to-pathway network was applied to reveal communities of connected pathways. PathWalks exploits a map that we construct in the form of a synthetic gene network, containing integrated information regarding a disease of interest. For our calculations we used the multi-thread version of PathWalks with 15 walkers, 10000 steps per walker and restart every 50 steps run in the infrastructure provided by the National Initiatives for Open Science in Europe – NI4OS Europe (https://ni4os.eu/ni4os-europe-vs-covid19/). Using the resulting pathway frequencies *i.e.* number of visits per pathway, we performed an odds ratio analysis with respect to a random walk of the pathway network using only the topology of the network without any gene guidance. Specifically, we defined the odds ratio between guided to non-guided walks as:

$$OR = \frac{\frac{P_i^G}{\left(1-P_i^G\right)}}{\frac{P_i^T}{\left(1-P_i^T\right)}} \quad (12)$$

$$P_i^{G/T} = \frac{F_i^{G/T}}{F_t^{G/T}} \quad i \in \{1,2 \dots n\} \quad (13)$$

Where index G and T denote the variables corresponding to the guided and topology-only runs, respectively. $P_i^{G/T}$ is the visiting probability of the i^{th} pathway calculated as the frequency F_i ratio over the total visits F_t^T o*n* pathways. According to this analysis pathways with OR values greater than 1 are the ones with higher relative visiting frequency compared to the topology-only runs, and are thus more likely to be involved in the disease of interest. On the other hand, *OR* values less than 1 correspond to pathways that are less relevant.

Pathways with OR values greater than one were visualized as a network using R's igraph package[89], highlighting specific pathways of interest.

CoDRes reranking and drug lists unification and scoring

The top 50 host-targeting drugs from the 10 lists (Supplementary File 3) were used as input to the CoDReS tool[22]. CoDReS combines an initial drug ranking that may be the repurposing score or an *a priori* score, with a functional score of each drug results from the analysis of the disease of interest, as well as with a structural score derived from drugability violations. Specifically, the initial ranking score of each host-targeted drug from the 10 lists divided with the absolute maximum ranking score, was used as the normalized a-priori repurposing score for CoDReS. Furthermore, for the case of functional and structural scores the 1001 genes from the integration analysis were used with their disease association scores and the structures (SMILES format) of each drug respectively. A composite score (CoDRes score) was calculated, for each drug, as the normalized weighted sum of the initial *a priori* score (aS) with a functional (FS) and a structural score (StS). The weights that determine the desired influence of each part to the final score, were defined as w_{aS} =0.45, w_{FS} =0.45 and w_{StS} =0.1.

Chemical structure diversity analysis and clustering

We searched and downloaded the structures of the 240 drugs from PubChem[91], CLUE - The Drug Repurposing Hub[92](https://clue.io/repurposing#download-data) and from the literature. We removed (i) duplicates entries (drugs found in more than one list), (ii) drugs for which we did not find a structure and (iii) elemental entries (*i.e.* copper). We then used the OpenBabel software[93] to convert the structures of the remaining 210 drugs to a single sdf library file which was then used as input in the ChemBioServer 2.0 tool[23] for calculating the distance matrix of their chemical and structural similarity.

Comparison with running clinical trials

All listed clinical studies related to the coronavirus disease (COVID-19) were collected from the ClinicalTrials.gov. Small-molecule drugs curated through the reported clinical studies and the 2D-structures of the drugs (sdf files) were obtained from PubChem (https://pubchem.ncbi.nlm.nih.gov/), where available.

The sdf file containing the chemical structures of the integrated list of 65 drugs and all the available structures of the drugs reported in currently running clinical trials was used as an input to Chembioserver 2.0 in order to obtain the corresponding Tanimoto distance matrix. The latter was analysed in R to identify which proposed drugs have the same or similar compounds in clinical trials using a distance threshold of <= 0.2.

Supplementary Material

Supplementary File 1: Top 150 over- and under-expressed genes/proteins/metabolites – regulators

Supplementary File 2: GWAS analysis

Supplementary File 3: Top 50 and Top 20 drug lists

Supplementary File 4: Integration Scores

Supplementary File 5: Complete antiviral drugs from TaxAV and HPAV

Supplementary File 6: Detailed table of the top 65 drugs

Acknowledgments

M.T., G.M., M.Z., A.O., A.K., M.Z., C.C., G.M.S. were funded by the European Commission Research Executive Agency Grant BIORISE [number 669026], under the Spreading Excellence, Widening Participation, Science with and for Society Framework.

E.K. was funded by the State Scholarships Foundation (IKY) scholarship, under the Action 'Strengthening Human Resources, Education and Lifelong Learning', 2014–2020; co-funded by the European Social Fund (ESF) and the Greek State [MIS-5000432]. M.M.B. is funded by the State Scholarships Foundation (IKY) scholarship; co-financed by Greece and the European Union (European Social Fund- ESF) through the Operational Programme «Human Resources Development, Education and Lifelong Learning» in the context of the project 'Reinforcement of Post-doctoral Researchers - 2nd Cycle' [MIS-5033021], implemented by the State Scholarships Foundation (IKY).

Numerical simulations were run on the PARADOX-IV supercomputing facility at the Scientific Computing Laboratory, National Center of Excellence for the Study of Complex Systems, Institute of Physics Belgrade, supported in part by the Ministry of Education, Science, and Technological Development of the Republic of Serbia under project No. ON171017.

Author Contributions

G.M.S. conceived and supervised the study. M.B., A.K., C.C. and G.M.S. collected, curated and analyzed the RNA-Seq, Proteomics and Metabolomics datasets. E.L. Performed and analyzed the GWAS-phenotypic analysis. M.Z. and G.M.S. developed and performed the multi-omic integration approach. G.M., M.T. and M.B. developed, performed and analyzed the pathogen-host interaction and taxonomy-based drug repurposing approach. K.S., M.B., and M.T. collected the chemical structures for all compounds of interest,

performed the structural diversity analysis and comparison of the identified drugs with the ongoing clinical trials. E.K., M.T. and G.M.S. performed and analyzed the PathWalks results for the functional analysis of the genes of interest. N.D. annotated the integrated drug list with the relevant chemical data along with the MeSH, TBC and Chem classifications. Expert's curation, annotation and discussion on highlighted drugs was performed by N.D., G.K. and T.K. Figures, tables and supplementary information were prepared by M.T., M.B., M.Z., G.M., N.D. and G.M.S.; M.T., M.B., M.Z., G.M., E.L., A.K., C.C., K.S., N.D., T.K. and G.M.S. wrote the manuscript while all authors contributed in editing and reviewing. A.O, S.A., M. Zanti., A. Onisiforou., J.R., C.G.C., T.K., N.D. and G.K. provided feedback on various aspects of the work. All authors have read and approved the submitted version of the manuscript.

Conflicts of Interest

The authors declare no conflict of interest.

References

1. Pushpakom, S. *et al.* Drug repurposing: Progress, challenges and recommendations. *Nature Reviews Drug Discovery* (2018). doi:10.1038/nrd.2018.168

2. Jose, R. J. & Manuel, A. COVID-19 cytokine storm: the interplay between inflammation and coagulation. *The Lancet Respiratory Medicine* (2020). doi:10.1016/S2213-2600(20)30216-2

3. Zhou, S., Wang, Y., Zhu, T. & Xia, L. CT features of coronavirus disease 2019 (COVID-19) pneumonia in 62 patients in Wuhan, China. *Am. J. Roentgenol.* (2020). doi:10.2214/AJR.20.22975

4. Guo, T. *et al.* Cardiovascular Implications of Fatal Outcomes of Patients with Coronavirus Disease 2019 (COVID-19). *JAMA Cardiol.* (2020). doi:10.1001/jamacardio.2020.1017

5. Shen, B. *et al.* Proteomic and Metabolomic Characterization of COVID-19 Patient Sera. *Cell* (2020). doi:10.1016/j.cell.2020.05.032

6. Blanco-Melo, D. *et al.* SARS-CoV-2 launches a unique transcriptional signature from in vitro, ex vivo, and in vivo systems. *Cell* (2020). doi:10.1101/2020.03.24.004655

7. Xiong, Y. *et al.* Transcriptomic characteristics of bronchoalveolar lavage fluid and peripheral blood mononuclear cells in COVID-19 patients. *Emerg. Microbes Infect.* (2020). doi:10.1080/22221751.2020.1747363

8. Gordon, D. E. *et al.* A SARS-CoV-2 protein interaction map reveals targets for drug repurposing. *Nature* (2020). doi:10.1038/s41586-020-2286-9

9. Thul, P. J. *et al.* A subcellular map of the human proteome. *Science (80-.).* (2017). doi:10.1126/science.aal3321

10. Subramanian, A. *et al.* A Next Generation Connectivity Map: L1000 Platform and the First 1,000,000 Profiles. *Cell* (2017). doi:10.1016/j.cell.2017.10.049

11. Duan, Q. *et al.* L1000CDS2: LINCS L1000 characteristic direction signatures search engine. *npj Syst. Biol. Appl.* (2016). doi:10.1038/npjsba.2016.15

12. Wang, Z., Lachmann, A., Keenan, A. B. & Ma'Ayan, A. L1000FWD: Fireworks visualization of drug-induced transcriptomic signatures. *Bioinformatics* (2018). doi:10.1093/bioinformatics/bty060

13. Wang, Z. *et al.* Extraction and analysis of signatures from the Gene Expression Omnibus by the crowd. *Nat. Commun.* (2016). doi:10.1038/ncomms12846

14. Staley, J. R. *et al.* PhenoScanner: A database of human genotype-phenotype associations. *Bioinformatics* (2016). doi:10.1093/bioinformatics/btw373

15. Kamat, M. A. *et al.* PhenoScanner V2: An expanded tool for searching human genotype-phenotype associations. *Bioinformatics* (2019). doi:10.1093/bioinformatics/btz469

16. Cotto, K. C. *et al.* DGIdb 3.0: A redesign and expansion of the drug-gene interaction database. *Nucleic Acids Res.* (2018). doi:10.1093/nar/gkx1143

17. Wishart, D. S. DrugBank: a comprehensive resource for in silico drug discovery and exploration. *Nucleic Acids Res.* (2006). doi:10.1093/nar/gkj067

18. Wishart, D. S. *et al.* DrugBank 5.0: A major update to the DrugBank database for 2018. *Nucleic Acids Res.* (2018). doi:10.1093/nar/gkx1037

19. Zachariou, M., Minadakis, G., Oulas, A., Afxenti, S. & Spyrou, G. M. Integrating multi-source information on a single network to detect disease-related clusters of molecular mechanisms. *J. Proteomics* (2018). doi:10.1016/j.jprot.2018.03.009

20. Zuberi, K. *et al.* GeneMANIA prediction server 2013 update: biological network integration for gene prioritization and predicting gene function. *Nucleic Acids Res.* (2013). doi:10.1093/nar/gkt533

21. Karatzas, E. *et al.* PathWalks: identifying pathway communities using a disease-related map of integrated information. *Bioinformatics* (2020). doi:10.1093/bioinformatics/btaa291

22. Karatzas, E., Minadakis, G., Kolios, G., Delis, A. & Spyrou, G. M. A Web Tool for Ranking Candidate Drugs Against a Selected Disease Based on a Combination of Functional and Structural Criteria. *Comput. Struct. Biotechnol. J.* (2019). doi:10.1016/j.csbj.2019.05.010

23. Karatzas, E. *et al.* ChemBioServer 2.0: an advanced web server for filtering, clustering and networking of chemical compounds facilitating both drug discovery and repurposing. *Bioinformatics* (2020). doi:10.1093/bioinformatics/btz976

24. Schomburg, D. & Schomburg, I. SARS coronavirus main proteinase 3.4.22.69 BT - Class 3.4–6 Hydrolases, Lyases, Isomerases, Ligases: EC 3.4–6. in (eds. Schomburg, D. & Schomburg, I.) 65–97 (Springer Berlin Heidelberg, 2013). doi:10.1007/978-3-642-36260-6_3

25. Lu, I. L. *et al.* Structure-based drug design and structural biology study of novel nonpeptide inhibitors of severe acute respiratory syndrome coronavirus main protease. *J. Med. Chem.* (2006). doi:10.1021/jm060207o

26. Ghosh, A. K. *et al.* Structure-based design, synthesis, and biological evaluation of a series of novel and reversible inhibitors for the severe acute respiratory syndrome - Coronavirus papain-like protease. *J. Med. Chem.* (2009). doi:10.1021/jm900611t

27. Chaudhuri, R. *et al.* Comparison of SARS and NL63 papain-like protease binding sites and binding site dynamics: Inhibitor design implications. *J. Mol. Biol.* (2011). doi:10.1016/j.jmb.2011.09.030

28. Jacobs, J. *et al.* Discovery, synthesis, and structure-based optimization of a series of N-(tert-butyl)-2-(N-arylamido)-2-(pyridin-3-yl) acetamides (ML188) as potent noncovalent small molecule inhibitors of the severe acute respiratory syndrome coronavirus (SARS-CoV) 3CL pr. *J. Med. Chem.* **56**, 534–546 (2013).

29. Deaton, D. N., Graham, K. P., Gross, J. W. & Miller, A. B. Thiol-based angiotensin-converting enzyme 2 inhibitors: P1' modifications for the exploration of the S1' subsite. *Bioorganic Med. Chem. Lett.* (2008). doi:10.1016/j.bmcl.2008.01.046

30. Huentelman, M. J. *et al.* Sructure-based discovery of a novel angiotensin-converting enzyme 2 inhibitor. *Hypertension* (2004). doi:10.1161/01.HYP.0000146120.29648.36

31. Husain, M. & Cheung, C.-Y. Histone Deacetylase 6 Inhibits Influenza A Virus Release by Downregulating the Trafficking of Viral Components to the Plasma Membrane via Its Substrate, Acetylated Microtubules. *J. Virol.* (2014). doi:10.1128/jvi.00727-14

32. Triplett, T. A., Holay, N., Kottapalli, S., VanDenBerg, C. & Capasso, A. Elucidating the Role of HDACs in T Cell Biology and Comparing Distinct HDAC Inhibitors in Augmenting Responses to Cancer Immunotherapy. *J. Immunol.* **204**, 165.23 LP-165.23 (2020).

33. Akimova, T., Beier, U. H., Liu, Y., Wang, L. & Hancock, W. W. Histone/protein deacetylases and T-cell immune responses. *Blood* **119**, 2443–2451 (2012).

34. Weisberg, E. *et al.* Repurposing of Kinase Inhibitors for Treatment of COVID-19. *Pharm. Res.* **37**, 167 (2020).

35. Dyall, J. *et al.* Repurposing of clinically developed drugs for treatment of Middle East respiratory syndrome coronavirus infection. *Antimicrob. Agents Chemother.* (2014). doi:10.1128/AAC.03036-14

36. Mulgaonkar, N. *et al.* Bcr-Abl tyrosine kinase inhibitor imatinib as a potential drug for COVID-19. *bioRxiv* 2020.06.18.158196 (2020). doi:10.1101/2020.06.18.158196

37. Xing, J. *et al.* Reversal of Infected Host Gene Expression Identifies Repurposed Drug Candidates for COVID-19. *bioRxiv Prepr. Serv. Biol.* (2020). doi:10.1101/2020.04.07.030734

38. Bermejo, M. *et al.* Dasatinib inhibits HIV-1 replication through the interference of SAMHD1 phosphorylation in CD4+ T cells. *Biochem. Pharmacol.* (2016). doi:10.1016/j.bcp.2016.02.002

39. Ramaiah, M. J. mTOR inhibition and p53 activation, microRNAs: The possible therapy against pandemic COVID-19. *Gene Reports* (2020). doi:10.1016/j.genrep.2020.100765

40. Omarjee, L. *et al.* Targeting T-cell senescence and cytokine storm with rapamycin to prevent severe progression in COVID-19. *Clinical Immunology* (2020). doi:10.1016/j.clim.2020.108464

41. Campbell, G. R. *et al.* Induction of autophagy by PI3K/MTOR and PI3K/MTOR/BRD4 inhibitors suppresses HIV-1 replication. *J. Biol. Chem.* **293**, 5808–5820 (2018).

42. Mao, L. *et al.* Neurologic Manifestations of Hospitalized Patients with Coronavirus Disease 2019 in Wuhan, China. *JAMA Neurol.* (2020). doi:10.1001/jamaneurol.2020.1127

43. Kopel, J., Perisetti, A., Gajendran, M., Boregowda, U. & Goyal, H. Clinical Insights into the Gastrointestinal Manifestations of COVID-19. *Digestive Diseases and Sciences* (2020). doi:10.1007/s10620-020-06362-8

44. Ma, L., Song, K. & Huang, Y. Coronavirus Disease-2019 (COVID-19) and Cardiovascular Complications. *Journal of Cardiothoracic and Vascular Anesthesia* (2020). doi:10.1053/j.jvca.2020.04.041

45. Zheng, Y. Y., Ma, Y. T., Zhang, J. Y. & Xie, X. COVID-19 and the cardiovascular system. *Nature Reviews Cardiology* (2020). doi:10.1038/s41569-020-0360-5

46. Ye, Z., Zhang, Y., Wang, Y., Huang, Z. & Song, B. Chest CT manifestations of new coronavirus disease 2019 (COVID-19): a pictorial review. *Eur. Radiol.* (2020). doi:10.1007/s00330-020-06801-0

47. Li, H. *et al.* Serum Amyloid A is a biomarker of severe Coronavirus Disease and poor prognosis. *J. Infect.* (2020). doi:10.1016/j.jinf.2020.03.035

48. Lo, M. W., Kemper, C. & Woodruff, T. M. COVID-19: Complement, Coagulation, and Collateral Damage. *J. Immunol.* (2020). doi:10.4049/jimmunol.2000644

49. Saxena, A. *et al.* A lung transcriptomic analysis for exploring host response in COVID-19. *J. Pure Appl. Microbiol.* (2020). doi:10.22207/JPAM.14.SPL1.47

50. Hondermarck, H., Bartlett, N. W. & Nurcombe, V. The role of growth factor receptors in viral infections: An opportunity for drug repurposing against emerging viral diseases such as COVID-19? *FASEB BioAdvances* (2020). doi:10.1096/fba.2020-00015

51. Tutuncuoglu, B. *et al.* The Landscape of Human Cancer Proteins Targeted by SARS-CoV-2. *Cancer discovery* (2020). doi:10.1158/2159-8290.CD-20-0559

52. Hoffmann, M. *et al.* SARS-CoV-2 Cell Entry Depends on ACE2 and TMPRSS2 and Is Blocked by a Clinically Proven Protease Inhibitor. *Cell* (2020). doi:10.1016/j.cell.2020.02.052

53. McGee, M. C., August, A. & Huang, W. BTK/ITK dual inhibitors: Modulating immunopathology and lymphopenia for COVID-19 therapy. *Journal of Leukocyte Biology* (2020). doi:10.1002/JLB.5COVR0620-306R

54. Roschewski, M. *et al.* Inhibition of Bruton tyrosine kinase in patients with severe COVID-19. *Sci. Immunol.* **5**, (2020).

55. Rivera-Torres, J. & José, E. S. Src tyrosine kinase inhibitors: New perspectives on their immune, antiviral, and senotherapeutic potential. *Front. Pharmacol.* (2019). doi:10.3389/fphar.2019.01011

56. Branchford, B. R. *et al.* The small-molecule MERTK inhibitor UNC 2025 decreases platelet activation and prevents thrombosis. *J. Thromb. Haemost.* **16**, 352–363 (2018).

57. Piegeler, T. *et al.* Ropivacaine attenuates endotoxin plus hyperinflation-mediated acute lung injury via inhibition of early-onset Src-dependent signaling. *BMC Anesthesiol.* (2014). doi:10.1186/1471-2253-14-57

58. Li, L. F. *et al.* Nintedanib reduces ventilation-augmented bleomycin-induced epithelial–mesenchymal transition and lung fibrosis through suppression of the Src pathway. *J. Cell. Mol. Med.* (2017). doi:10.1111/jcmm.13206

59. Li, L. F. *et al.* Mechanical ventilation augments bleomycin-induced epithelial-mesenchymal transition through the Src pathway. *Lab. Investig.* (2014). doi:10.1038/labinvest.2014.75

60. Oyaizu, T. *et al.* Src tyrosine kinase inhibition prevents pulmonary ischemia-reperfusion- induced acute lung injury. *Intensive Care Med.* (2012). doi:10.1007/s00134-012-2498-z

61. Grillet, F., Behr, J., Calame, P., Aubry, S. & Delabrousse, E. Acute Pulmonary Embolism Associated with COVID-19 Pneumonia Detected with Pulmonary CT Angiography. *Radiology* (2020). doi:10.1148/radiol.2020201544

62. Dupont, V. *et al.* Excess soluble fms-like tyrosine kinase 1 correlates with endothelial dysfunction and organ failure in critically ill COVID-19 patients. *Clin. Infect. Dis.* (2020). doi:10.1093/cid/ciaa1007

63. Marchetti, M. COVID-19-driven endothelial damage: complement, HIF-1, and ABL2 are potential pathways of damage and targets for cure. *Annals of Hematology* (2020). doi:10.1007/s00277-020-04138-8

64. Perla, A. *et al.* Histone Deacetylase Inhibitors in Pediatric Brain Cancers: Biological Activities and Therapeutic Potential. *Frontiers in Cell and Developmental Biology* (2020). doi:10.3389/fcell.2020.00546

65. Sanjib Banerjee, N., Moore, D. W., Broker, T. R. & Chow, L. T. Vorinostat, a pan-HDAC inhibitor, abrogates productive HPV-18 DNA amplification. *Proc. Natl. Acad. Sci. U. S. A.* (2018). doi:10.1073/pnas.1801156115

66. Acosta, Y. Y., Montes-Casado, M. & Aragoneses, L. Erratum: Suppression of CD4+ T lymphocyte activation 'in vitro' and experimental encephalomyelitis 'in vivo' by the phosphatidyl inositol 3-kinase inhibitor PIK-75 (International Journal of Immunopathology and Pharmacology (2014) 27:1 (53-67)). *International Journal of Immunopathology and Pharmacology* (2015). doi:10.1177/0394632015572738

67. Wei, K. *et al.* Nerve growth factor protects the ischemic heart via attenuation of the endoplasmic reticulum stress induced apoptosis by activation of phosphatidylinositol 3-kinase. *Int. J. Med. Sci.* (2015). doi:10.7150/ijms.10101

68. Eastman, R. T. *et al.* Remdesivir: A Review of Its Discovery and Development Leading to Emergency Use Authorization for Treatment of COVID-19. *ACS Cent. Sci.* (2020). doi:10.1021/acscentsci.0c00489

69. Verschueren, K. H. G. *et al.* A Structural View of the Inactivation of the SARS Coronavirus Main Proteinase by Benzotriazole Esters. *Chem. Biol.* (2008). doi:10.1016/j.chembiol.2008.04.011

70. Bacha, U. *et al.* Development of broad-spectrum halomethyl ketone inhibitors against coronavirus main protease 3CLpro. *Chem. Biol. Drug Des.* (2008). doi:10.1111/j.1747-0285.2008.00679.x

71. Zhang, H., Penninger, J. M., Li, Y., Zhong, N. & Slutsky, A. S. Angiotensin-converting enzyme 2 (ACE2) as a SARS-CoV-2 receptor: molecular mechanisms and potential therapeutic target. *Intensive Care Med.* (2020). doi:10.1007/s00134-020-05985-9

72. Robinson, M. & McCarthy…, D. edgeR: differential expression analysis of digital gene expression data. *Bioconductor.Fhcrc.Org* (2010).

73. Love, M. I., Huber, W. & Anders, S. Moderated estimation of fold change and dispersion for RNA-seq data with DESeq2. *Genome Biol.* (2014). doi:10.1186/s13059-014-0550-8

74. Krämer, A., Green, J., Pollard, J. & Tugendreich, S. Causal analysis approaches in ingenuity pathway analysis. *Bioinformatics* (2014). doi:10.1093/bioinformatics/btt703

75. Gkogkou, E., Barnasas, G., Vougas, K. & Trougakos, I. P. Expression profiling meta-analysis of ACE2 and TMPRSS2, the putative anti-inflammatory receptor and priming protease of SARS-CoV-2 in human cells, and identification of putative modulators. *Redox Biol.* 101615 (2020).

76. Kerrien, S. *et al.* The IntAct molecular interaction database in 2012. *Nucleic Acids Res.* (2012). doi:10.1093/nar/gkr1088

77. Durmuş Tekir, S. *et al.* PHISTO: Pathogen-host interaction search tool. *Bioinformatics* (2013). doi:10.1093/bioinformatics/btt137

78. Guirimand, T., Delmotte, S. & Navratil, V. VirHostNet 2.0: surfing on the web of virus/host molecular interactions data. *Nucleic Acids Res.* **43**, D583–D587 (2015).

79. Buniello, A. *et al.* The NHGRI-EBI GWAS Catalog of published genome-wide association studies, targeted arrays and summary statistics 2019. *Nucleic Acids Res.* (2019). doi:10.1093/nar/gky1120

80. Psaty, B. M. *et al.* Cohorts for Heart and Aging Research in Genomic Epidemiology (CHARGE) Consortium design of prospective meta-analyses of genome-wide association studies from 5 Cohorts. *Circulation: Cardiovascular Genetics* (2009). doi:10.1161/CIRCGENETICS.108.829747

81. Federhen, S. The NCBI Taxonomy database. *Nucleic Acids Res.* (2012). doi:10.1093/nar/gkr1178

82. Chamberlain, S. A. & Szöcs, E. Taxize: Taxonomic search and retrieval in R. *F1000Research* (2013). doi:10.12688/f1000research.2-191.v2

83. Clarke, K. R. & Warwick, R. M. A taxonomic distinctness index and its statistical properties. *J. Appl. Ecol.* (1998). doi:10.1046/j.1365-2664.1998.3540523.x

84. Clarke, K. R. & Warwick, R. M. A further biodiversity index applicable to species lists: Variation in taxonomic distinctness. *Mar. Ecol. Prog. Ser.* (2001). doi:10.3354/meps216265

85. Spellerberg, I. F. & Fedor, P. J. A tribute to Claude-Shannon (1916-2001) and a plea for more rigorous use of species richness, species diversity and the 'Shannon-Wiener' Index. *Glob. Ecol. Biogeogr.* (2003). doi:10.1046/j.1466-822X.2003.00015.x

86. Shannon, C. E. The Mathematical Theory of Communication. *M.D. Comput.* (1997). doi:10.2307/410457

87. Carlson, M. org. Hs. eg. db: Genome Wide Annotation for Human. R package version 3.2. 3. (2019).

88. Paul Shannon, 1 *et al.* Cytoscape: A Software Environment for Integrated Models of Biomolecular Interaction Networks. *Genome Res.* (2003). doi:10.1101/gr.1239303.metabolite

89. Hunter, J. E. & Cohen, S. H. Package: igraph. *Educ. Psychol. Meas.* **29**, 697–700 (2007).

90. R Development Core Team. R: A language and environment for statistical computing. *Vienna, Austria* (2018). doi:R Foundation for Statistical Computing, Vienna, Austria. ISBN 3-900051-07-0, URL http://www.R-project.org.

91. Bolton, E. E., Wang, Y., Thiessen, P. A. & Bryant, S. H. Chapter 12 PubChem: Integrated Platform of Small Molecules and Biological Activities. in *Annual Reports in Computational Chemistry* (2008). doi:10.1016/S1574-1400(08)00012-1

92. Corsello, S. M. *et al.* The Drug Repurposing Hub: A next-generation drug library and information resource. *Nature Medicine* (2017). doi:10.1038/nm.4306

93. O'Boyle, N. M. *et al.* Open Babel: An Open chemical toolbox. *J. Cheminform.* (2011). doi:10.1186/1758-2946-3-33

Figure Legends

Figure 1. Overview of the workflow. A) Multi-omics datasets were selected from various sources in order to identify differentially expressed genes, differentially abundant metabolites and proteins along with protein-protein interactions (PPIs) between SARS-CoV-2 and other pathogens with the human host. This was followed by B) Multiplex drug repurposing approaches based on i) transcriptomics, ii) GWAS – Phenotype association analysis iii) pathogen–host Interaction network analysis, and C) Integration of the multi-omic data from patients for D) Reranking the drug candidates based on the calculated target-disease association of the integration map. E) The structural similarity of candidate drugs was calculated to cluster the top scoring compounds. Finally, the integrated drug list comprises 65 drugs out of which 16 were manually curated by experts for further annotation.

Figure 2. Taxonomy tree of all the pathogens used in the host-pathogen interaction drug repurposing approaches. The main taxonomic groups are highlighted with light blue slices showing the ancestral taxonomy groups for SARS-CoV-2 (Green leaf). The yellow to red colored bars represent the number of drugs obtained from various taxa. The circular blue to yellow heat map represents the number of pathogen-host protein interactions retrieved from various databases.

Figure 3. Integrated of multi-omic patient data. network along with the distributions of the weighted degree, weighted gene-specific information and the combined MIG scores. Node size represents the MIG score bin for each gene while colors indicate the originating omics dataset. Nodes with mixed colors show genes commonly identified from different datasets. The bar plot shows the MIG score for each gene as the weighted sum of Edge (yellow) and Nodal (blue) scores. The subplots show the corresponding distributions.

Figure 4. Connected pathway communities related to COVID-19 on a pathway-to-pathway network as highlighted by PathWalks. The bar plot shows the odds ratio value for the top 30 KEGG pathways, found to be involved in COVID-19. The bar plot color scale represents the visit counts from less (dark blue) to more (light) frequently visited pathways.

Figure 5. Sankey plots of the drugs highlighted after expert curation of integrated list in Table 2. Drugs are ordered based on their normalized ranking and pathways based on their OR value obtained from PathWalks. (A) Drugs targeting human pathways, their originating list, their target genes and corresponding pathways. (B) Antiviral drugs targeting viral proteins, their originating list and known target pathogens.

Tables

Table 1. Summary of the 12 drug lists generated from all repurposing pipelines

List ID	Source DATA	Drug DB	Main Pipeline Methods & Tools	Description
Tr1	RNA-Seq Series1,2&5,6,7	LINCS L1000	Connectivity Map, L1000CDS2, L1000FWD	Drugs aiming at reversing the gene expression profile induced by COVID-19.
TrC1	RNA-Seq Series1,2&5,6,7	Drug Matrix (GSE5992)	CREEDS	
Tr2	RNA-Seq - Series 15	LINCS L1000	Connectivity Map, L1000CDS2, L1000FWD	
TrC2	RNA-Seq - Series 15	Drug Matrix (GSE5992)	CREEDS	
Tr3	RNA-Seq - BALF	LINCS L1000	Connectivity Map, L1000CDS2, L1000FWD	
TrC3	RNA-Seq - BALF	Drug Matrix (GSE5992)	CREEDS	
Tr4	RNA-Seq - PBMC	LINCS L1000	Connectivity Map, L1000CDS2, L1000FWD	
TrC4	RNA-Seq - PBMC	Drug Matrix (GSE5992)	CREEDS	
GW	GWAS	DGIdb	Phenoscanner	Drugs targeting host proteins from genes with significant SNP-phenotypic association with COVID-19
HPH	PPI, NCBI	DrugBank	In-house methods	Drugs targeting host proteins found to interact with SARS-CoV-2 proteins and/or other pathogens
HPAV	PPI, NCBI	DrugBank	In-house methods	Drugs targeting pathogen proteins - direct antiviral activity
TaxAV	NCBI	DrugBank	In-house methods	

Table 2: The integrated list of 65 drugs ranked by the highest normalized ranking. The classification of the listed drugs was based on three classification systems; MeSH (Medical Subject Headings), TBC (Target-Based Classification) and Chem (Chemical classification). Currently, active clinical trials that involve drugs in this list are noted (clinicaltrials.gov, last accessed on August 24th, 2020). A group of drugs that fulfilled specific criteria was selected by expert curation.

Drug	Max Rank	Classifications	Related Clinical Trials	Expert Selection
Dexamethasone	1.00	MeSH: Anti-inflammatory; Corticosteroid TBC: Steroid Hormone Receptor Agonist Chem: Steroid	**Clinical Trials:** 26 **Structurally similar in clinical trials:** methylprednisolone	
Atorvastatin	1.00	MeSH: Anticholesteremic TBC: Cholesterol synthesis Inhibitor Chem: Pyrrole	**Clinical Trials:** 4	
Beta-estradiol	1.00	MeSH: Estrogen TBC: Estrogen receptor agonist Chem: Steroid	**Clinical Trial:** 1	
Vorinostat	1.00	MeSH: Antineoplastic TBC: Histone deacetylase inhibitor Chem: Anilide		✓
Olanzapine	1.00	MeSH: Atypical antipsychotic TBC: 5-HT ligand; D2 dopamine receptor ligand; Histamine receptor ligand Chem: Heterocyclic; Benzodiazepine		
Cyclosporin-a	1.00	MeSH: Immunosuppressive TBC: Calcineurin inhibitor Chem: Cyclic peptide	**Clinical Trials:** 6	
Rosiglitazone	1.00	MeSH: Hypoglycemic agent TBC: Peroxisome proliferator-activated receptor Chem: Thiazole; Thiazolidinedione		
Bosutinib	1.00	MeSH: Antineoplastic agent TBC: Src tyrosine kinase inhibitor Chem: Aromatic amine; Aniline aminoquinoline		✓
Zinc acetate	1.00	MeSH: Antibacterial agent TBC: - Chem: Acetate		
Benzyl (2-oxopropyl) carbamate	1.00	MeSH: - TBC: SARS-CoVreplicase polyprotein 1ab inhibitor; 3 clpro protease inhibitor Chem: Benzyloxycarbonyl; Ketone		✓
Remdesivir	1.00	MeSH: Antiviral TBC: Adenine nucleotide analogue Chem: Aromatic amine	**Clinical Trials:** 48	✓
Dasatinib	0.95	MeSH: Antineoplastic TBC: Src Tyrosine kinase inhibitor Chem: Aromatic amine; Thiazoles, aminopyrimidine		✓
Mercaptopurine	0.95	MeSH: Antineoplastic; Immunomodulatory agent; Antimetabolite TBC: Purine analogue; Enzyme inhibitor Chem: Sulfhydryl compound; Aryl thiol; Purine analogue		
D3F	0.95	MeSH: Enzyme inhibitor TBC: SARS replicase polyprotein 1a inhibitor Chem: Nitrobenzene; Toluene; Trifluoromethylbenzene		✓
Raloxifene	0.95	MeSH: Antineoplastic; Bone Density Conservation agent TBC: Hormone;Selectiveestrogen receptor modulator; Estrogen antagonist Chem: Aromatic cyclic amino compound; Benzylidene.		
Cytarabine	0.95	MeSH: Antineoplastic; Immunosuppressive; Antimetabolite; Antiviral TBC: Pyrimidine analogue; Tyrosine protein kinase Src inhibitor; protease inhibitor Chem: Heterocycle; Pyrimidine; Arabinonucleoside		✓
Imatinib	0.95	MeSH: Antineoplastic TBC: Tyrosine kinase inhibitor Chem: Benzamides; Aromatic amine	**Clinical Trials:** 5	✓
Selumetinib	0.89	MeSH: - Anti-neurofibromatosis type 1 TBC: MAP kinase inhibitor; MEK inhibitor Chem: Secondary amino; Benzimidazole		
Azd-8055	0.89	MeSH: Experimental antiproliferative TBC: Phosphatidyl inositol 3' kinase-related kinase inhibitor; Voltage-gated potassium channel ligand; Rapamycin kinase inhibitor Chem: Oxazine; Morpholine		
Avrainvillamide-analog-3	0.89	MeSH: Antiproliferative TBC: Nuclear chaperone nucleophosmin ligand Chem: Alkaloid		
Linsitinib	0.89	MeSH: Antineoplastic		

		TBC: Insulin receptor inhibitor; Insulin-like growth factor-I receptor inhibitor; Type II Receptor tyrosine kinase inhibitor Chem: Pyrazines; Quinoline		
Fluocinoloneacetonide	0.89	MeSH: Anti-inflammatory TBC: Steroid Hormone Receptor Agonist Chem: Steroid; Alcohol; Ketone	**Structurally similar in clinical trials:** Budesonide	
Dobutamine	0.89	MeSH: Sympathomimetic; Cardiac stimulant TBC: Adrenergic beta-1 Receptor Agonist Chem: Catecholamine; secondary amine		
Bromfenac	0.89	MeSH: NSAID TBC: COX inhibitor Chem: Ketone; Benzophenones; Aromatic amine; Anilines;		
Testosterone	0.89	MeSH: Hormone, Androgen, Anabolic TBC: Sex hormone receptor agonist Chem: Steroid; Androgen	**Structurally similar in clinical trials:** Hydrocortisone	
Hydroxychloroquine	0.89	MeSH: Antiparasitic agent, Antimalarial, Antirheumatic agent TBC: Enzyme inhibitor, heme polymerase inhibitor, endosomes modulator, toll-like receptors inhibitor Chem: Aromatic amine; Aminoquinoline	**Clinical Trials:** 250 **Structurally similar in clinical trials:** hydroxychloroquine sulfate, chloroquine, chloroquine phosphate	
Hydroxyurea	0.89	MeSH: Antineoplastic agent, Antimetabolite, Antisickling agent TBC: Nucleic acid synthesis inhibitor; Ribonucleoside-diphosphate reductase inhibitor Chem: Urea		
F3F	0.89	MeSH:- TBC: SARS-CoV replicase polyprotein 1ab inhibitor Chem: Furan; Triazole		✓
Daunorubicin	0.84	MeSH: Antineoplastic; Antibacterial TBC: Topoisomerase II Inhibitor Chem: Aminoglycosides; Anthracyclines; Cyclic ketone, Acenoquinone		
PD-0325901	0.84	MeSH: Experimental antineoplastic TBC: MAPK inhibitor Chem: Benzamide		
Zidovudine	0.84	MeSH: Antiviral agent, Antimetabolite TBC: Nucleoside and Nucleotide Reverse Transcriptase Inhibitor Chem: Glycoside; Pyrimidine; Dideoxynucleosides		
GRL0617	0.84	MeSH:- TBC: SARS-CoVreplicase polyprotein 1ab inhibitor Chem: Carboxylic acid nitrile; cyano compound; peptide		✓
AG-14361	0.84	MeSH:- TBC: Poly ADP-ribose polymerase 1 inhibitor Chem: Benzodiazepine; Benzimidazole		
Dactolisib (nvp-bez235)	0.84	MeSH: Antineoplastic TBC: Phosphatidyl inositol 3' kinase-related kinase inhibitor; Lipid modifying kinase inhibitor Chem: Imidazole; Imidazoquinoline	**Clinical Trial:** 1	✓
Carboplatin	0.84	MeSH: Antineoplastic TBC: Aquation agent Chem: Coordination Complex; Platinum compound		
Zileuton	0.84	MeSH: NSAID TBC: Leukotriene antagonist; Lipoxygenase Inhibitor Chem: Urea; Benzothiophene		
Staurosporine	0.84	MeSH: Multi-enzyme inhibitor TBC: Protein kinase C inhibitor; CAMK2 inhibitor; Death-associated kinase inhibitor; Phosphorylase kinase inhibitor; Tyrosine-(Y)-phosphorylation regulated kinase inhibitor; Acetylcholine receptor ligand Chem: Indole; indolocarbazole alkaloid		
Fasudil	0.79	MeSH: Peripheral vasodilators TBC: ROCK inhibitor; DMPK kinase inhibitor; Calcium Channel Blocker Chem: Sulfonamides		
GSK-1059615	0.79	MeSH:- TBC: Enzyme inhibitor, PI3K inhibitor Chem: Pyridine; quinoline; thiazolidinone		
PI 103 hydrochloride	0.79	MeSH:- TBC: AGC protein kinase inhibitor; PKC inhibitor; CMGC protein kinase inhibitor; tyrosine protein kinase inhibitor Chem: Pyrimidine		
Hexachlorophene	0.79	MeSH: Anti-infective agent, Antiseptic TBC:- Chem: Chlorobenzene; Chlorophenol		
Ofloxacin	0.79	MeSH: Antibacterial; Antineoplastic TBC: Topoisomerase IV inhibitor Chem: Aromatic amine; N-arylpiperazine; quinolone	**Clinical Trial:** 1	
Leflunomide	0.79	MeSH: Antirheumatic agent	**Clinical Trials:** 2	

		TBC: Nucleoside synthesis inhibitor; oxidoreductase inhibitor Chem: Isoxazole		
Prasterone	0.79	MeSH: Anabolic steroid, hormone TBC: Estrogen receptor agonist; androgen receptor agonist; GABAa antagonist, NMDA agonist Chem: Steroid		
N-(2-aminoethyl)-1-aziridineethanamine	0.79	MeSH: Experimental antiviral agent TBC: ACE2 inhibitor Chem: Aziridine		✓
Triptolide	0.79	MeSH: Antineoplastic alkylating agent; antispermatogenic agent; immunosuppressive agent, TBC: Multiprotein inhibitor Chem: Terpene; phenanthrenes; diterpenes; diterpenoid		
WR1	0.79	MeSH:- TBC: Inhibitor for the Major Protease of the SARS Coronavirus Chem: Benzyloxycarbonyl; benzyloxycarbonyl		✓
Y-27632	0.74	MeSH: Neuromuscular; muscle relaxant; antihypertensive agent; Enzyme inhibitor TBC: Rho kinase inhibitor, protein kinase N inhibitor. Chem: Pyridine; aromatic amide		
DG8735000	0.74	MeSH:- TBC: Inhibitor of ultraviolet mediated damage Chem: Aminobenzoate		
Saracatinib	0.74	MeSH: Antineoplastic agent; enzyme inhibitor TBC: Src inhibitor; tyrosine kinase inhibitor Chem: Benzodioxoles; quinazoline		✓
LY-255283	0.74	MeSH: Antiasthmatic agent TBC: Leukotriene Antagonists Chem: Tetrazoles; aromatic ketone		
Rofecoxib	0.74	MeSH: NSAID; Analgesic non-narcotic agent TBC: COX2 inhibitor Chem: Lactone; furan; butanolide		
Simvastatin	0.74	MeSH: Antimetabolite; anticholesteremic; hypolipidemic TBC: Hydroxymethylglutaryl-CoA Reductase Inhibitor Chem: Polycyclic aromatic; naphthalene; fatty acid ester	**Clinical Trials:** 4	
Ebastine	0.74	MeSH: Antihistamine TBC: H1 antagonist Chem: Piperidine; ketone, butyrophenone		
Cisplatin	0.74	MeSH: Antineoplastic; radiation-sensitizing agent TBC: DNA replication inhibition Chem: Platinum compound		
Hydroquinone	0.74	MeSH: Antioxidant; radiation-protective agent TBC: Melanin Synthesis Inhibitor; HDAC inhibitor Chem: Phenol; benzenediol		✓
Calcium citrate	0.74	MeSH: Anticoagulant TBC: Calcium chelating agent Chem: Tricarboxylic acid derivative		
JAK3-IN-1	0.68	MeSH:- TBC: AGC protein kinase inhibitor; tyrosine kinase inhibitor Chem: Heterocyclic compound		
Pracinostat	0.68	MeSH: Experimental antineoplastic TBC: Histone deacetylase inhibitor Chem: Benzimidazole		
Blebbistatin	0.68	MeSH:- TBC: Myosin inhibitor Chem: Tertiary alcohol; ketone; pyrroloquinoline		
Pioglitazone	0.68	MeSH: Hypoglycemic agent (antidiabetic) TBC: Peroxisome proliferator-activated receptor-gamma activator Chem: Azole; thiazole; thiazolidinedione	**Clinical Trials:** 2	
Tegafur	0.68	MeSH: Antimetabolite; Antineoplastic; Immunosuppressive TBC: Thymidylate synthase inhibitor Chem: Pyrimidine; fluorouracil		
Choline salicylate	0.68	MeSH: NSAID, analgesic non-narcotic TBC: COX inhibitor Chem: Acid; benzoate; salicylate, phenol; hydroxybenzoic acid		
Methotrexate	0.68	MeSH: Antimetabolite; antineoplastic; abortifacient; immunosuppressive; antirheumatic TBC: Folic acid metabolism inhibitor; nucleic acid synthesis inhibitor Chem: Acid; pterin; aminopterin	**Clinical Trials:** 3 **Structurally similar in clinical trials:** folic acid	✓
Clofibrate	0.68	MeSH: Hypolipidemic; Anticholesteremic TBC: Peroxisome proliferator-activated receptor-gamma inhibitor Chem: Clofibric Acid; ethyl ester		

D3F: *2-[(2,4-Dichloro-5-Methylphenyl)Sulfonyl]-1,3-Dinitro-5-(Trifluoromethyl)Benzene*
F3F: *S-[5-(Trifluoromethyl)-4H-1,2,4-Triazol-3-YL] 5-(Phenylethynyl)Furan-2-Carbothioate*
GRL0617: *5-amino-2-methyl-N-[(1R)-1-naphthalen-1-ylethyl]benzamide*
WR1: *Nalpha-[(Benzyloxy)Carbonyl]-N-[(1R)-4-Hydroxy-1-Methyl-2-Oxobutyl]-L-Phenylalaninamide*
DG8735000: *4-(Dimethylamino)benzoic acid*

Table 3. Summary of the data along with the source study

Source/Study Method	*List ID*	*Sample Description*	*Controls vs Infected*		*Selected Differentially Expressed Genes Proteins & Metabolites*			
			Con.	**Inf.**	**Adj. P-val threshold**	**logFC**	**Over**	**Under**
RNA-Seq / Transcriptomics GSE147507[6]	Series 1	Independent biological triplicates of primary human lung epithelium (NHBE) were mock treated or infected with SARS-CoV-2	3	3	<0.05	>=1	94	15
	Series 2 & 5	Both Series 2 and series 5 have Independent biological triplicates of transformed lung alveolar (A549) cells that were mock treated or infected with SARS-CoV-2	6	6	<0.05	>=1	147	9
	Series 6	Independent biological triplicates of transformed lung alveolar (A549) transduced with a vector expressing human **ACE2**, were mock treated or infected with SARS-CoV-2	3	3	<0.05	>=1	1083	352
	Series 7	Independent biological triplicates of transformed lung-derived Calu-3 cells were mock treated or infected with SARS-CoV-2	3	3	<0.05	>=1	1264	660
	Series 15	Uninfected human lung biopsies from two patients and used as biological replicates. Additionally, lung samples derived from a single male COVID-19 deceased patient processed in **technical** replicates.	2	2	<0.05	>=1	515	3838
RNA-Seq / Transcriptomics [7]	BALF	Bronchoalveolar lavage fluid (BALF) samples from Zhongnan Hospital of Wuhan University	3	2	< 1e-10	>=2	679	325
	PBMC	Peripheral blood mononuclear cells (PBMC) specimens of COVID-19 patients	3	3	< 0.01	>=1	707	316
LC-MS / Proteomics[5]	SerumP	COVID-19 patients' sera and healthy individuals	28	28	< 0.05	>0.25	62	58
GC-MS / Proteomics[5]	SerumM	COVID-19 patients' sera and healthy individuals	28	28	< 0.05	>0.25	97	317

Figures

Figure 1.

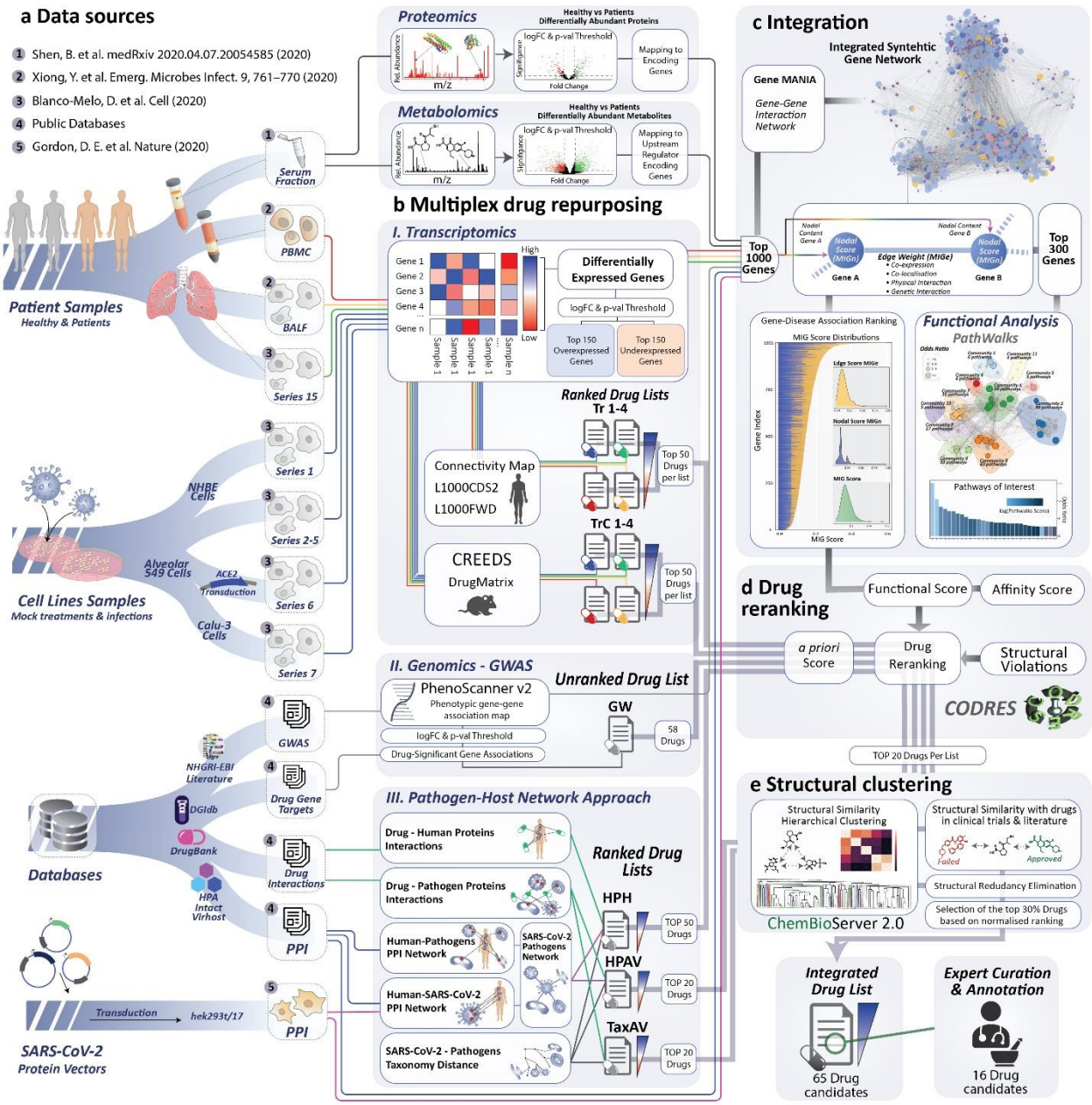

Figure 2

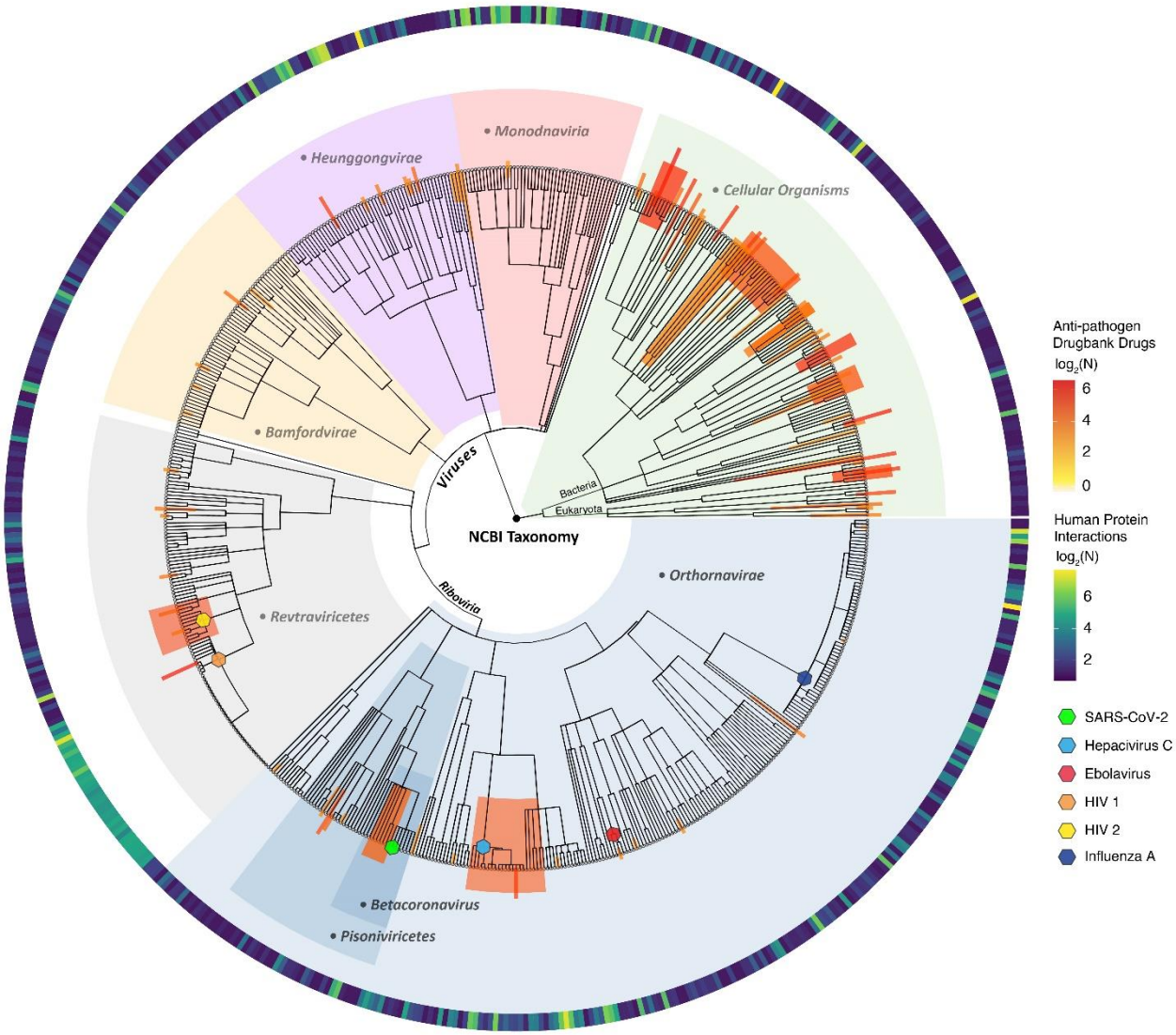
• Monodnaviria
• Heunggongvirae
• Cellular Organisms
• Bamfordvirae
Viruses
Bacteria
Eukaryota
NCBI Taxonomy
• Orthornavirae
Riboviria
• Revtraviricetes
• Betacoronavirus
• Pisoniviricetes
Anti-pathogen Drugbank Drugs
log2(N)
6
4
2
0
Human Protein Interactions
log2(N)
6
4
2
SARS-CoV-2
Hepacivirus C
Ebolavirus
HIV 1
HIV 2
Influenza A

Figure 3

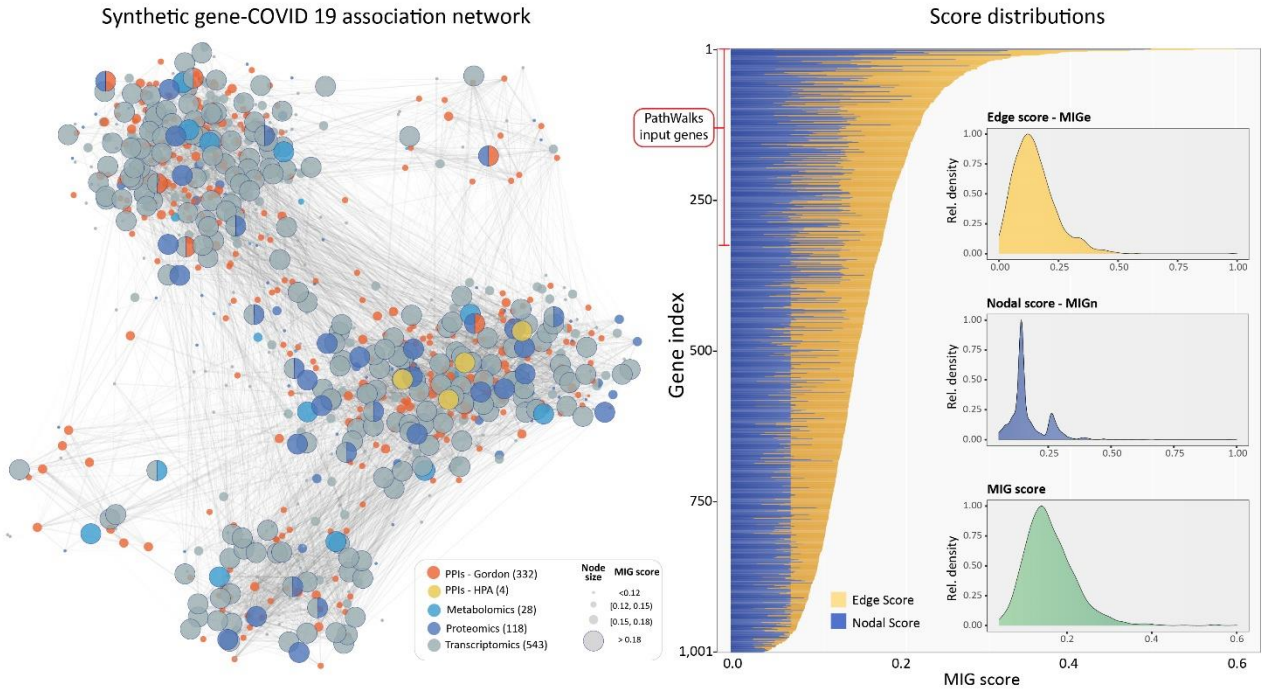
Synthetic gene-COVID 19 association network
Score distributions
PPIs - Gordon (332)
PPIs - HPA (4)
Metabolomics (28)
Proteomics (118)
Transcriptomics (543)
Node size
MIG score
<0.12
[0.12, 0.15)
[0.15, 0.18)
> 0.18
PathWalks input genes
Gene index
1
250
500
750
1,001
Edge Score
Nodal Score
0.0
0.2
0.4
0.6
MIG score
Edge score - MIGe
Nodal score - MIGn
MIG score
Rel. density

Figure 4

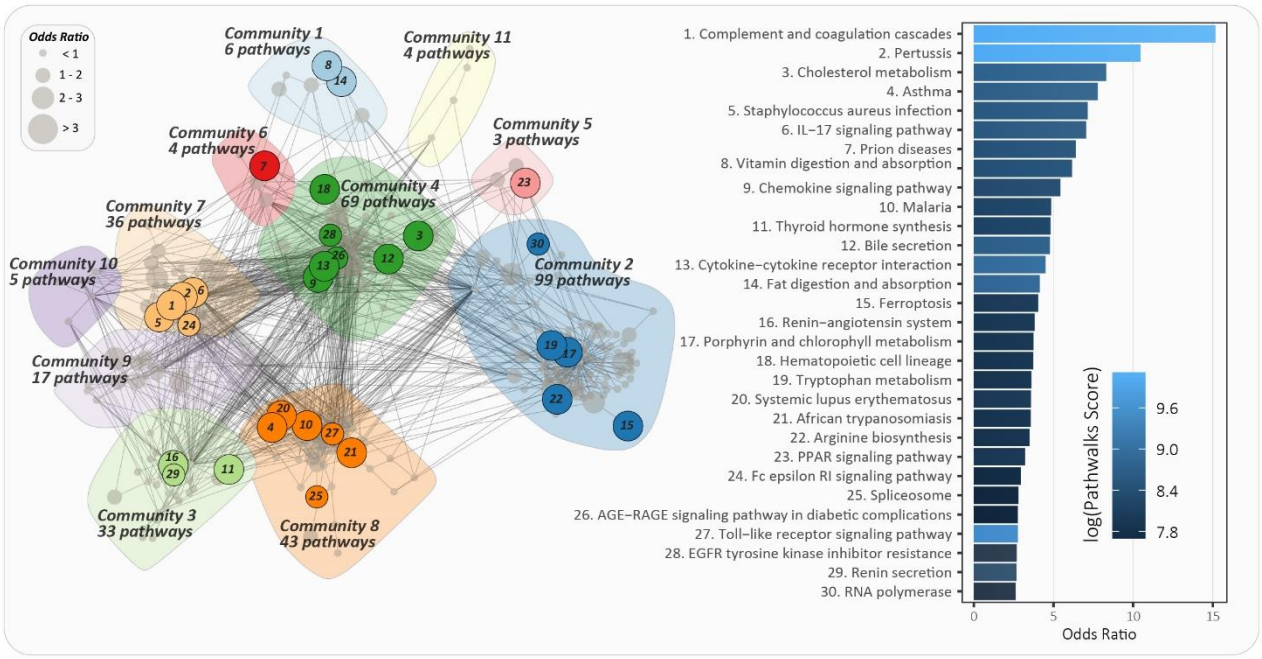
Odds Ratio
< 1
1 - 2
2 - 3
> 3
Community 1
6 pathways
Community 11
4 pathways
Community 6
4 pathways
Community 5
3 pathways
Community 4
69 pathways
Community 7
36 pathways
Community 10
5 pathways
Community 2
99 pathways
Community 9
17 pathways
Community 3
33 pathways
Community 8
43 pathways
1. Complement and coagulation cascades
2. Pertussis
3. Cholesterol metabolism
4. Asthma
5. Staphylococcus aureus infection
6. IL−17 signaling pathway
7. Prion diseases
8. Vitamin digestion and absorption
9. Chemokine signaling pathway
10. Malaria
11. Thyroid hormone synthesis
12. Bile secretion
13. Cytokine−cytokine receptor interaction
14. Fat digestion and absorption
15. Ferroptosis
16. Renin−angiotensin system
17. Porphyrin and chlorophyll metabolism
18. Hematopoietic cell lineage
19. Tryptophan metabolism
20. Systemic lupus erythematosus
21. African trypanosomiasis
22. Arginine biosynthesis
23. PPAR signaling pathway
24. Fc epsilon RI signaling pathway
25. Spliceosome
26. AGE−RAGE signaling pathway in diabetic complications
27. Toll−like receptor signaling pathway
28. EGFR tyrosine kinase inhibitor resistance
29. Renin secretion
30. RNA polymerase
log(Pathwalks Score)
9.6
9.0
8.4
7.8
0
5
10
15
Odds Ratio

Figure 5

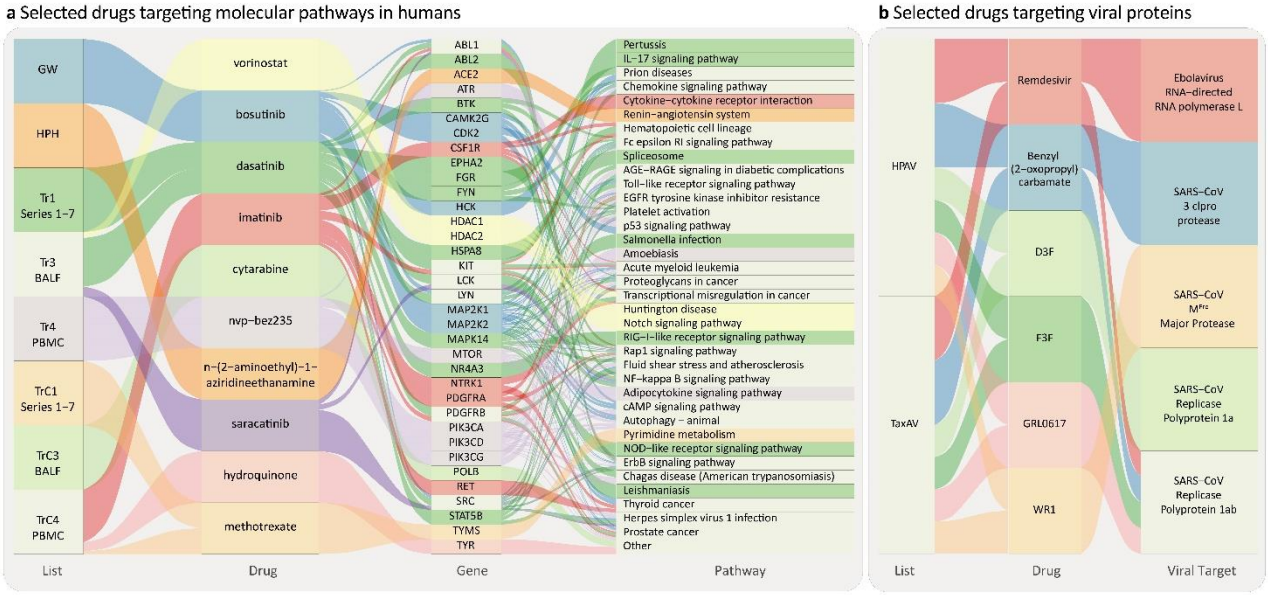
a Selected drugs targeting molecular pathways in humans
GW
HPH
Tr1 Series 1–7
Tr3 BALF
Tr4 PBMC
TrC1 Series 1–7
TrC3 BALF
TrC4 PBMC
vorinostat
bosutinib
dasatinib
imatinib
cytarabine
nvp–bez235
n–(2–aminoethyl)–1–aziridineethanamine
saracatinib
hydroquinone
methotrexate
ABL1
ABL2
ACE2
ATR
BTK
CAMK2G
CDK2
CSF1R
EPHA2
FGR
FYN
HCK
HDAC1
HDAC2
HSPA8
KIT
LCK
LYN
MAP2K1
MAP2K2
MAPK14
MTOR
NR4A3
NTRK1
PDGFRA
PDGFRB
PIK3CA
PIK3CD
PIK3CG
POLB
RET
SRC
STAT5B
TYMS
TYR
Pertussis
IL–17 signaling pathway
Prion diseases
Chemokine signaling pathway
Cytokine–cytokine receptor interaction
Renin–angiotensin system
Hematopoietic cell lineage
Fc epsilon RI signaling pathway
Spliceosome
AGE–RAGE signaling in diabetic complications
Toll–like receptor signaling pathway
EGFR tyrosine kinase inhibitor resistance
Platelet activation
p53 signaling pathway
Salmonella infection
Amoebiasis
Acute myeloid leukemia
Proteoglycans in cancer
Transcriptional misregulation in cancer
Huntington disease
Notch signaling pathway
RIG–I–like receptor signaling pathway
Rap1 signaling pathway
Fluid shear stress and atherosclerosis
NF–kappa B signaling pathway
Adipocytokine signaling pathway
cAMP signaling pathway
Autophagy – animal
Pyrimidine metabolism
NOD–like receptor signaling pathway
ErbB signaling pathway
Chagas disease (American trypanosomiasis)
Leishmaniasis
Thyroid cancer
Herpes simplex virus 1 infection
Prostate cancer
Other
List
Drug
Gene
Pathway
b Selected drugs targeting viral proteins
HPAV
TaxAV
Remdesivir
Benzyl (2–oxopropyl) carbamate
D3F
F3F
GRL0617
WR1
Ebolavirus RNA–directed RNA polymerase L
SARS–CoV 3 clpro protease
SARS–CoV Mpro Major Protease
SARS–CoV Replicase Polyprotein 1a
SARS–CoV Replicase Polyprotein 1ab
List
Drug
Viral Target